United States Naval Postgraduate School

THESIS

HEAT TRANSFER CONSIDERATIONS IN A PRESSURE VESSEL BEING CHARGED

by

John Thomas Lyons III

June 1969

102

Heat Transfer Considerations in a Pressure Vessel Being Charged

by

John Thomas Lyons III
Lieutenant (junior grade), United States Navy
B.S., United States Naval Academy, 1968

Submitted in partial fulfillment of the
requirements for the degree of

MASTER OF SCIENCE IN MECHANICAL ENGINEERING

from the
NAVAL POSTGRADUATE SCHOOL
June 1969

Author John T. Lyons III

Approved by: Robert H. Nunn
Thesis Advisor

Chairman, Department of Mechanical Engineering

R. F. Rinehart
Academic Dean

ABSTRACT

Experimental data for the charging of an air receiver is presented and interpreted in detail. The data indicates a substantial departure from the adiabatic behavior. The experimental results are used to evaluate existing closed form expressions for the thermodynamic state of a gas in a receiver. A method for experimentally determining the convective heat transfer coefficient is developed, evaluated and used in conjunction with these expressions.

The experimental work was performed from March 1969 through May 1969 at the Naval Postgraduate School, Monterey, California.

TABLE OF CONTENTS

LIST OF TABLES

LIST OF ILLUSTRATIONS

PRECEDING PAGE BLANK

ACKNOWLEDGMENT

The author wishes to express gratitude to Professor R. H. Nunn for his assistance and advice throughout the investigation both in the design of the test equipment and in the interpretation of results. A debt of gratitude is also owed to Messrs. H. Perry and R. Garcia for their work in the construction and installation of the experimental equipment.

I. INTRODUCTION

Systems using the charging of a receiver are often employed today. A common practice when analyzing a receiver being charged is to assume that the process is adiabatic. This simplifies the governing equations for the system and leads to a fairly straightforward expression for the state of the gas in the vessel. During the course of the charging process however, a substantial temperature difference between the walls of the receiver and the gas in the receiver may develop. Often the tank's thermal capacitance is of sufficient magnitude to permit the extraction of large amounts of energy from the gas with only a small change in the temperature at the outside surface of the tank walls. This obscures the apparent effect of heat transfer, for the absence of a noticeable temperature change at the outside of the receiver walls may lend credence to the adiabatic assumption whereas actually large amounts of heat are being transferred from the gas to the receiver walls. Errors introduced by such an assumption may lead to serious problems. For example, if heat transfer is neglected, calculations for determining the amount of gas needed to charge a vessel may lead to a predicted value lower than that actually required.

In order to aid in the analysis of this problem Reynolds [Ref. 1] developed a theory which includes the effects of heat transfer for determining the thermodynamic state of gas in a receiver during the charging process. He developed four

closed form solutions for the various magnitudes of the system parameters. Using his criteria to determine the proper closed form solution, many charging processes may be analyzed without excessive difficulty. The accuracy of these solutions depends to a great extent on the accuracy with which the average convective heat transfer coefficients can be estimated for the charging process.

In his experimental investigation of the blowdown process [Ref. 2] Reynolds tested his theory using an $\bar{h}$ (average convective heat transfer coefficient for the entire blowdown process) determined by taking the value of his heat transfer parameter NTU (number of thermal units, see Appendix A) which when used in his theoretical equation of state gave the best fit to the experimental data. These $\bar{h}$ values were on the order of those predicted on the basis of an assumption of steady state turbulent free convection inside the receiver, i.e.,

$$\frac{hL}{k} = .13(GRPR)^{1/3} \quad .$$

Therefore Reynolds suggested the use of an $\bar{h}$ based on this assumption in his solution to the charging process.

The problem still remains, however, that unless $\bar{h}$ is determined by an independent means it is difficult to come to any quantitative conclusions as to the accuracy of Reynolds' theory.

The purpose of this study has been to derive a method for experimentally determining the average convective heat transfer coefficient between the gas and the receiver, and to

apply these results to three of Reynolds' closed form solutions in order to evaluate their accuracy. The three closed form solutions evaluated are for conditions where the heat transfer from the receiver walls to the surrounding medium can be neglected. These three cases are the ones most commonly encountered. The fourth of these closed form solutions deals with the case where the walls of the receiver are very thin and the heat transfer from the receiver walls to the ambient medium must be taken into account. This solution was not evaluated due to the difficulties in experimentally determining the average convective heat transfer coefficient between the walls of the receiver and the surrounding medium. Also presented in this paper are representative values for the various heat transfer parameters determined in this undertaking.

In the following sections of this thesis the theoretical and analytical methods and results are discussed. Following a description of the charging system, the theoretical model due to Reynolds is reviewed and the methods for the experimental evaluation of the heat transfer coefficient are developed. The experimental results are then discussed in the light of their relevance to Reynolds' model and their usefulness in engineering problems. A final section is included in order to summarize this work and indicate some areas for future investigation.

II. OBJECTIVES

Experiments on the charging of a gas receiver were conducted at varying flow rates and heat transfer environments, in order to accomplish the following objectives:

(1) Evaluate the closed form solutions developed by Reynolds to approximate the thermodynamic state of a gas during charging.

(2) Develop, use, and evaluate an expression for experimentally determining the average instantaneous heat transfer coefficient in a gas receiver being charged.

III. DESCRIPTION OF EXPERIMENTAL APPARATUS

A. GENERAL DESCRIPTION

The test apparatus (Figures 1 through 4) consisted of an aluminum cylindrical gas receiver with a volume of 1.03 cubic feet. The complete physical dimensions of the test apparatus are listed in Table 1. The vessel was designed according to the ASME Boiler and Pressure Vessel Code for a working pressure of 200 psig. Its top was removable to allow access to the interior of the tank, using an O-Ring flange arrangement to insure airtightness when the top was in place. The receiver was fitted with a flow metering device mounted in the center of the tank top. The other fittings consisted of a mounting for a thermocouple probe, a pressure transducer mounting, and a bleed valve arrangement.

This test receiver was mounted so as to be immersed in a larger tank which was either open to the atmosphere or filled with ice water depending on the particular run. Air for charging the test tank was supplied from two 117 cubic foot air vessels charged by an air-cooled compressor. The supply pressure to the flow metering device was varied from 180 psig to 10 psig.

B. FLOW METERING

The mass flow rate for each run was determined by maintaining a critical flow through one of two nozzles or through an orifice. These small diameter (D) devices were machined from stainless steel in accordance with a paper by Grace and Lapple [Ref. 3] and the discharge coefficients (C_D) given in their paper were used in these calculations. The diameter and discharge coefficients are listed in Table 1. The orifice or nozzle was mounted on the tank top in a flange type arrangement that was sealed by O-Rings and connected to a 1 inch line that lead to the supply tanks. The stagnation pressure (P_0) was read by a local pressure tap and gage arrangement mounted just upstream of the flow metering device. The stagnation temperature (T_0) was likewise found by using a thermocouple mounted in the flow just upstream of the metering device. It should be noted here that for velocities of the magnitude occurring in these tests, it was safe to assume that the difference between stagnation and local conditions upstream of the orifice was negligible. Thus, assuming adiabatic flow through the orifice or nozzle, the temperature and pressure values of

P_0 and T_0 indicated by the apparatus just described can be used in the critical flow equation,

$$w = .532\ C_D \frac{\pi \frac{D^2}{4} P_0}{\sqrt{T_0}} \quad .$$

The air to the flow metering device was controlled by a quick acting Jamesbury ball valve.

C. TEMPERATURE MEASUREMENT

The test vessel was fitted with a thermocouple probe consisting of four 40-gage copper constantan thermocouples. The thermocouple housings were designed so as to measure as closely as possible the local temperature at four equally spaced heights in the receiver (Fig. 1). The thermocouples were arranged so that the four could be read in series, and, at the same time, any one of the four could be read independently. The series signal was recorded on channel one of a two channel Moseley strip chart recorder, while the signal of the thermocouple being read singly was recorded on a continuous Brown recorder. According to the manufacturer's specifications thermocouples of this type are accurate to within ±1.5°R for the temperature ranges found in these tests. Since the thermocouple probe readings were only used qualitatively, no further calibration was made. As was mentioned above, the stagnation temperature of the inlet air was read from a single thermocouple. The signal of this 40-gage copper constantan thermocouple was monitored on a Leeds and Northrup recorder.

D. PRESSURE MEASUREMENTS

The pressure in the test receiver was obtained by use of a Daystrom Wiancko pressure transducer attached to the receiver whose signal was recorded on channel two of the Moseley strip chart recorder. The input voltage (21 volts) to the transducer was supplied by a Philco power supply and the transducer output signal was adjusted so as to read 10 psi/in on the Moseley recorder. The pressure transducer was calibrated originally using a test gage and later using a dead-weight tester. When connected to the recorder the pressure transducer registered pressures within ± 1 psi of the actual pressure throughout the range of these tests.

IV. EXPERIMENTAL PROCEDURE

The experimental program was divided into the following three cases:

1. In the first group of runs the receiver was charged 12 times under conditions corresponding to the adiabatic case in Reynolds' theory. The runs consisted of three charges at each of four possible supply tank pressures; 190, 180, 170 and 160 psig. The 3/8 inch knife-edge orifice was mounted for these tests and the total elapsed time for a run was approximately one second. The large tank encircling the test receiver was open to the atmosphere. Thus the rapid chargings gave NTU values which dictated the use of Reynolds' adiabatic

model for theoretically determining the thermodynamic state of the gas in the receiver throughout the run (See Section V-A-3).

2. The second group of runs corresponded to the isothermal case described in Reynolds' theory. The 36 runs consisted of 3 runs at each of 12 possible supply tank pressures ranging from 180 psig to 10 psig, in various intervals. The 1/32 inch nozzle was mounted in the flow metering apparatus and the run time varied from 150 seconds to 75 seconds. Once again the large tank surrounding the test tank was open to the atmosphere. The resulting very small mass flow rates were introduced to correspond to NTU values in the region of 7, a lower limit for Reynolds' criteria.

3. The last set of runs was made with the test receiver completely immersed in ice water contained by the large tank. The first 9 runs were made with the 1/32 inch nozzle in place, three each at supply pressures of 180, 160 and 140 psig. The last 18 runs of this case were made with the 1/8 inch nozzle mounted in the tank top, three each at supply pressures of 180, 150, 120, 90, 60 and 30 psig. The ice bath was to maintain the receiver walls at a constant temperature and thus present the gas with an isothermal sink to correspond to the one described in the analytical model.

The values of the supply pressure listed above represent the nominal charging pressure. The actual stagnation pressure just upstream of the flow metering device was recorded for each run.

In making a series of runs, the supply tanks were first charged to approximately 190 psig. The system was then isolated from the compressor and the test receiver was allowed to reach equilibrium with its surrounding medium. The quick acting valve between the supply tanks and the flow metering device was then opened. It was kept open until the pressure in the test tank reached a value insufficient to maintain a critical pressure ratio across the flow meter. The valve was then closed and a run terminated. For the succeeding run the supply tank pressure was adjusted to the desired value and the test receiver was vented to the atmosphere. The next run did not commence until the temperature of the gas in the receiver (as indicated by the thermocouple probe) reached equilibrium with that of the tank walls and thus the surrounding medium. Having made one pass through the supply pressures indicated for a particular case, the supply tanks were recharged and the procedure repeated for a second and third time.

Throughout the charging process the pressure and temperature history of the gas in the tank was recorded on a two channel strip chart recorder.

V. THEORETICAL CONSIDERATIONS

A. THEORY DEVELOPED BY REYNOLDS[1]

1. Introduction

In an analysis of the charging process one object is to obtain the time dependent thermodynamic state of the gas in the receiver. A common practice is to express the temperature of the gas (the dependent variable) as a function of the mass (the independent variable). For a constant volume receiver the perfect gas law may then be used to express the pressure as a function of the mass. Knowing the mass flow rate the thermodynamic state of the gas as a function of time can be described.

With this in mind Reynolds developed the following model for a receiver being charged:

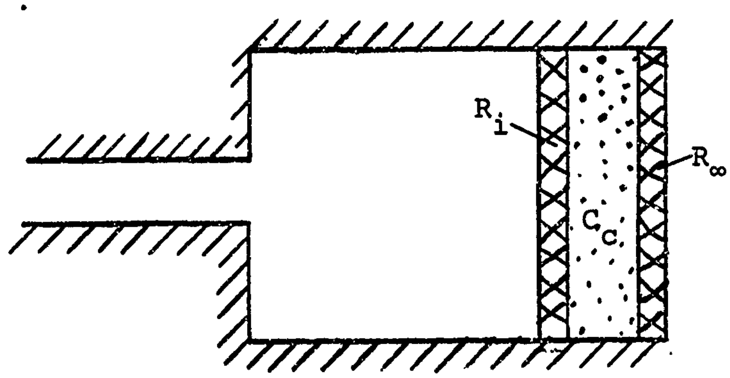

The thermal capacitance of the receiver walls and any other internal structure is lumped into a single capacitance

---

[1]The nomenclature used in this section is taken from Reference 1, see Appendix A for listing.

represented by C_c and equal to the product of the mass of the capacitance and its specific heat ($C_c = M_c c_p$). The heat transfer resistance between the receiver walls and the surrounding environment is represented by R_∞ and the heat transfer resistance between the capacitant material and the gas in the receiver is represented by R_i.

2. General Differential Equation for Charging

Reynolds assumes that the thermal resistance as well as the thermal capacitance are invariant with time. He also assumes perfect mixing of the injected gas and the gas in the receiver, and that the walls of the receiver are at a uniform temperature throughout. Using these assumptions he extends his model to include all the significant energy terms as follows:

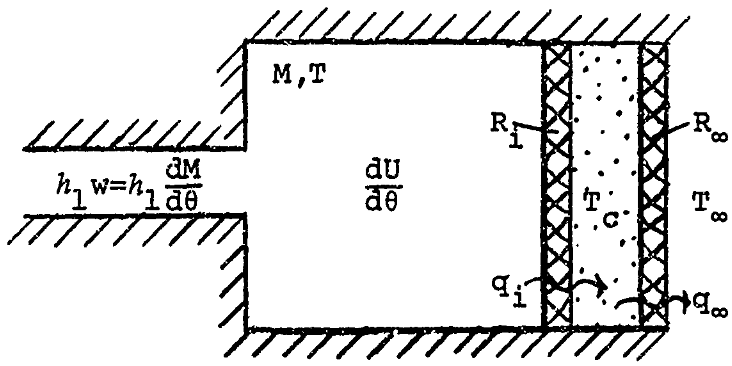

Combining an energy balance for the above model and the heat transfer rate equations,

$$q_\infty = \frac{T_c - T_\infty}{R_\infty} \qquad q_i = \frac{T - T_c}{R_i}$$

the following non-dimensional general differential equation for the charging is obtained (see Appendix B):

$$w^*M^* \frac{d^2T^*}{dM^{*2}} + w^*[2w^* + NTU + M^* \frac{dw^*}{dM^*} + \frac{NTU+NTU_\infty}{C_0^*} M^*]\frac{dT^*}{dM^*}$$

$$+ [w^* \frac{dw^*}{dM^*} + \frac{1}{C_0^*}(NTU+NTU_\infty)w^* + \frac{NTU\ NTU_\infty}{C_0^*}]T^*$$

$$- kT_1^*w^* \frac{dw^*}{dM^*} - \frac{NTU+NTU_\infty}{C_0^*} w^*kT_1^* - \frac{NTU\ NTU_\infty}{C_0^*} T_\infty^* = 0 \ .$$

For the case of constant mass flow rate ($w^* = 1$) this equation reduces to:

$$M^* \frac{d^2T^*}{dM^{*2}} + [C_1+C_2M^*]\frac{dT^*}{dM^*} + C_3T^* + C_4 = 0 \qquad (1)$$

where C_1, C_2, C_3, and C_4 are constants comprised of the system parameters NTU, NTU and C_0^*; defined as,

$$NTU = \frac{1}{R_i c_v w_0} = \frac{(hA)_i}{w_o c_v} \ ,$$

$$NTU_\infty = \frac{1}{R_\infty c_v w_0} = \frac{(hA)_\infty}{w_0 c_v}$$

and

$$C_0^* = \frac{M_c c_p}{M_0 c_v} = \frac{C_c}{M_0 c_v} \ .$$

The parameter NTU is used by Reynolds to represent the conductance (reciprocal of resistance) of the receiver as well as to give a measure of the rate of the process. The C_0^* parameter is the ratio of the capacitance of the receiver to the initial capacitance of the gas.

Reynolds solves equation (1) analytically, however the resulting series solution is seen to be impractical for many engineering applications. Fortunately in many cases the values of the system parameters are such that a simpler closed

form solution may be obtained. These solutions can be obtained by simplification of the series solution or by returning to the general differential equation for charging. In his report Reynolds nonetheless chooses to develop each closed form solution from a simplified form of his original model. A brief description of these and their solutions are presented in the following four sections. A complete derivation of the general differential equation for charging as well as derivations of the closed form solutions are presented in Appendix B.

3. Adiabatic Charging

As has been mentioned, a common method of analysis of a system being charged is to assume the process is adiabatic. This assumption of no heat transfer to or from the gas may be found to represent the case of a high mass flow rate charging (w_0 large) process fairly accurately. This may be thought of as due to the fact that the gas has not had time to transfer a substantial amount of heat to the walls before the charging process is terminated. Even if the high mass flow rate process is fairly lengthy, the effect of the heat transfer is small compared to the effect of introducing large quantities of mass during the charge. Such an assumption may also be justified for the case where the gas has been insulated from the thermal capacitance of the receiver walls ($h \simeq 0$). This case corresponds to the situation where NTU is very small, and the following model applies:

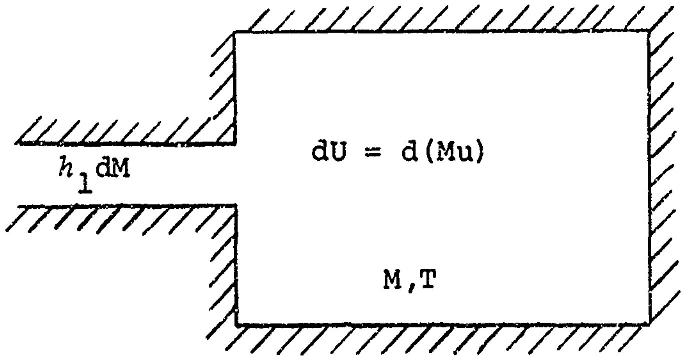

The solutions for the dimensionless temperature and pressure are,

$$T^* = kT_1^* - \frac{kT_1^*-1}{M^*} \tag{2}$$

and

$$P^* = kT_1^*(M^*-1) + 1 \quad . \tag{3}$$

4. <u>Isothermal Charging</u>

A receiver with a large thermal capacitance (C_c large) and either charged very slowly (w_0 small) or having a high hA value, will exhibit an isothermal behaviour. The normal temperature increase in the gas due to compression is not observed because the energy is extracted from the gas by the thermal capacitance of the receiver before it can become significant. As described above, a system of this type will have large values for the system parameters NTU and C_0*, and may be represented by the following model:

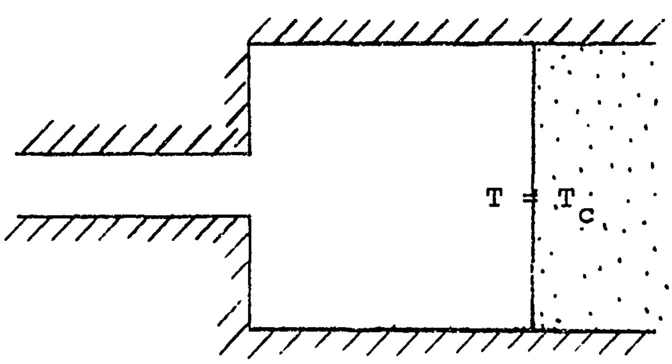

The temperature ratio for charging is by definition,

$$T^* = 1$$

and therefore,

$$P^* = M^* \quad .$$

5. Charging at Constant Mass Flow with Heat Transfer to an Isothermal Sink

In some systems the thermal capacitance of the wall is much larger than the thermal capacitance of the gas (C_0^* very large). For this case it can reasonably be assumed that the energy extracted from the gas is not great enough to significantly affect the temperature of the receiver walls (T_c is a constant). Thus the analytical model is modified to describe the heat transfer between the gas and an isothermal sink as follows:

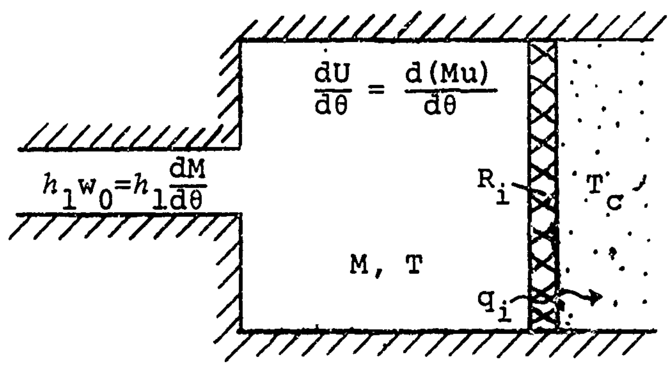

The solutions for this case are,

$$T^* = \frac{kT_1^* + NTUT_c^* - (kT_1^* - 1 - NTU + NTUT_c^*)M^{*-(1+NTU)}}{1+NTU} \quad (4)$$

and

$$P^* = \frac{(kT_1^* + NTUT_c^*)M^* - (kT_1^* - 1 - NTU + NTUT_c^*)M^{*-NTU}}{1+NTU} \quad . \quad (5)$$

6. Charging at Constant Mass Flow with Inside Resistance Negligible

A system having a high conductance can be assumed to have negligible inside heat transfer resistance (NTU high). This implies that the temperature of the capacitance is the same as that of the gas and the heat transfer is between the capacitance and the surrounding environment. That is distinguished from the isothermal case in that here the thermal capacitance is finite but not large (very thin walled cylinder for example). Since systems of this nature are not too common, Reynolds feels that the greatest value of this solution is that it supplies information for determining the effect of capacitance on the heat transfer in a charging process. The model for this system is:

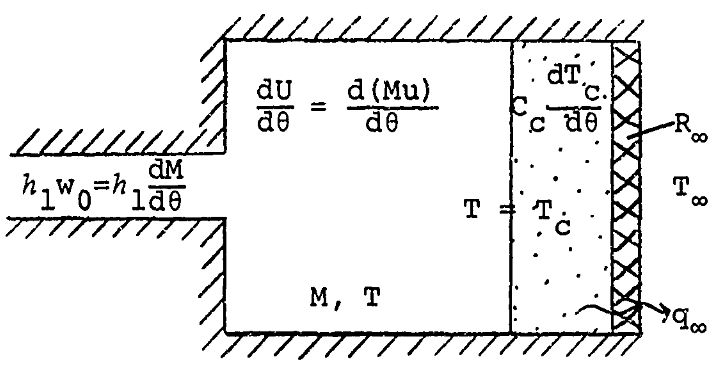

The solutions for this case are

$$T^* = \frac{(1+NTU_\infty - kT_1^* - NTU_\infty T_\infty^*)\left(\frac{C_0^*+1}{C_0^*+M^*}\right)^{1+NTU_\infty} + kT_1^* + NTU_\infty T_\infty^*}{1+NTU_\infty} \qquad (6)$$

and

$$P^* = T^*\left[(C_0^*+1)\left(\frac{1+NTU_\infty-kT_1^*-NTU_\infty T_\infty^*}{(1+NTU_\infty)T^*-kT_1^*-NTU_\infty T_\infty^*}\right)^{\frac{1}{1+NTU_\infty}}-C_0^*\right]. \quad (7)$$

B. CRITERIA FOR APPLICATION OF CLOSED FORM SOLUTIONS

In the previous four sections, closed form solutions were developed for the state of the gas in a receiver being charged. These solutions were developed by simplifying the original model with assumptions as to the magnitude and importance of various terms in the general solution. For example, in the adiabatic charging case the parameter NTU is assumed to be very small, thus the mass flow rate is large compared to the heat transfer coefficient and a solution based on no heat transfer is formulated. Similar types of assumptions are made for the other three cases. Reynolds then produces quantitative criteria for the use of such assumptions. These criteria are based on a maximum deviation of 5% in T* at the value of M* = 9. They are determined by comparing the case in question with the case which would give the maximum departure from this behavior. Thus the adiabatic case (no heat transfer to the walls) is compared to the case where the capacitance of the receiver walls is infinite, the isothermal sink case (large amounts of heat transfer to the walls). When the percentage T* difference between the two solutions is plotted against NTU, the value of the two solutions agree within 5% for values of NTU less than .25. In a similar

fashion criteria are developed for all the closed form solutions. Some solutions have more than one possible criteria for their use, however, only the criteria for the three cases tested here which are met by our experimental system are listed below. As mentioned before, the three closed form solutions evaluated here are the most useful and the criteria for their application are those most commonly found.

Adiabatic: $0 < NTU < 0.25$, all C_0^*

Isothermal Sink: $0.25 < NTU < 7$ $\quad C_0^* > 40$

Isothermal: $NTU > 7$ $\quad C_0^* > 40$.

C. DETERMINATION OF CONVECTIVE HEAT TRANSFER COEFFICIENT

In order to test Reynolds' theory on the state of a gas in a receiver being charged, a technique was devised to obtain a value for the convective heat transfer coefficient in the receiver in which the tests were run. To this end the following model of the experimental system was constructed:

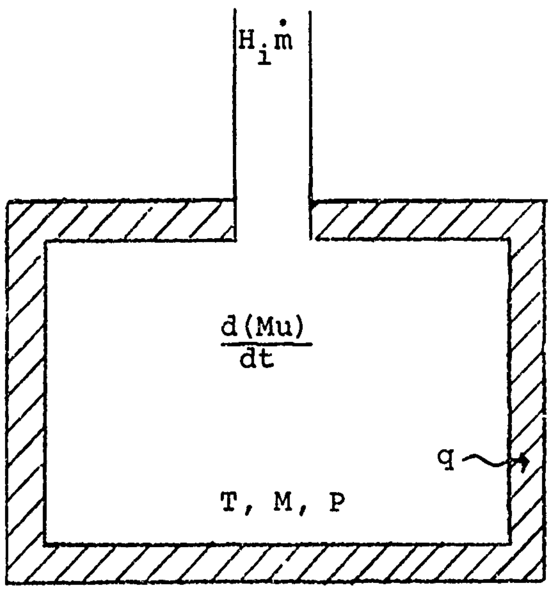

where,

$\dot{m}$ = the mass flow rate into the receiver

q = the heat transfer to the receiver walls

d(Mu)/dt = the rate of change of the internal energy of the gas in the receiver with respect to time

H_i = the stagnation enthalpy of the entering gas

T = the temperature of the gas in the receiver

P = the pressure of the gas in the receiver

M = the mass of the gas in the receiver .

Several points should be noted here. First it was assumed that the temperature throughout the receiver could be represented by a single value T (See discussion of imperfect mixing section V-E). The same was true for the pressure term P. It should also be noted that this development does not include the case where there is heat transfer between the surrounding medium and the walls of the receiver.

An energy balance on the receiver yields,

$$\dot{m}H_i - q = \frac{d(Mu)}{dt} \quad .$$

The kinetic energy of the gas in the receiver was neglected for it can be shown that for the flow rates in this experiment, the velocity of the gas in the receiver was very small when compared to the internal energy. Using the notation $\dot{f}$ to represent the derivative of a function f with respect to time, the above equation can be written as,

$$\dot{m}H_i - q = \dot{m}u + M\dot{u} \quad .$$

Assuming the gas in the receiver is thermallv and calorifically perfect,

$$q = -\dot{m}(c_v T - c_p T_i) - M c_v \dot{T} \tag{8}$$

where T_i is the inlet stagnation temperature of the gas. By definition of the convective heat transfer coefficient,

$$hA(T-T_w) = q = -Mc_v\dot{T} - \dot{m}(c_v T - c_p T_i) \quad .$$

In the same manner as T represents the average gas temperature, T_w is used to represent the average temperature of the receiver walls. Thus the h defined here represents an average instantaneous heat transfer coefficient for all points on the inside of the receiver walls. The symbol A represents the total inside area of the receiver walls. By use of the perfect gas law it can be seen that,

$$\frac{\dot{P}}{P} = \frac{\dot{m}}{M} + \frac{\dot{T}}{T}$$

for a constant volume system. Therefore the above equation can be written as,

$$h = \frac{-Mc_v T(\frac{\dot{P}}{P}) + \dot{m}c_p T_i}{A(T-T_w)}$$

or, using the perfect gas law again,

$$h = \frac{-c_v \dot{P}(\frac{V}{R}) + \dot{m}c_p T_i}{A[(\frac{PV}{MR}) - T_w]} \quad . \tag{9}$$

The next step was to determine an expression for T_w if it was not maintained a constant as in the isothermal sink case. In doing so the difficult task of determining experimentally an accurate average wall temperature was avoided. Since, for simplicity, no heat transfer from the outside of the receiver

walls to the surrounding medium was assumed, an energy balance on the walls yields,

$$q = \frac{d}{dt}(M_w u_w) = M_w C\dot{T}_w$$

where C is the specific heat of the walls and is assumed constant. Combining this with equation (8),

$$q = -\dot{m}(c_v T - c_p T_i) - Mc_v\dot{T} = M_w C\dot{T}_w$$

is obtained. Integrating this equation over time from t = 0 to t = t gives,

$$\int_{t=0}^{t=t} M_w C\dot{T}_w dt = \int_{t=0}^{t=t} [-\dot{m}(c_v T - c_p T_i) - Mc_v\dot{T}]dt$$

or

$$M_w C(T_w - T_{w_0}) = \int_{t=0}^{t=t} -\frac{d}{dt}(Mc_v T)dt + \int_{t=0}^{t=t} \dot{m}c_p T_i dt \quad .$$

In these tests T_i was a constant, therefore,

$$M_w C(T_w - T_{w_0}) = -Mc_v T + M_0 c_v T_0 + (M - M_0)c_p T_i$$

where subscript 0 denotes the condition at time t = 0.

Solving for T_w gives

$$T_w = \frac{-Mc_v T + M_0 c_v T_0 + Mc_p T_i - M_0 c_p T_i}{M_w C} + T_{w_0} \quad .$$

Again using the perfect gas law to eliminate the term T, the final form of the expression for T_w is obtained,

$$T_w = T_{w_0} + \left(\frac{M_0 c_p}{M_w C}\right)\left[\frac{M}{M_0}T_i - T\right] - \left(\frac{c_v V}{RM_w C}\right)[P - P_0] \quad . \qquad (10)$$

Equations (9) and (10) furnish a means for estimating the film coefficient h in terms of the tank pressure and gas mass and their rates. The massive experimental simplicity thus introduced is the major justification for the acceptance of

inaccuracies stemming from the definition of the heat transfer in terms of spacial averages of gas and wall properties.

D. DISCUSSION OF ASSUMPTION OF NO EXTERNAL HEAT TRANSFER

In the derivation of the expression for h it was assumed that there was no heat transfer from the outside of the receiver walls to the surrounding medium. This simplifies the energy balance, for if there is no heat transfer from the walls to the outside medium, all the energy leaving the gas must be stored in the receiver walls. This assumption is not only valid for this experimental system, but for many pressure vessels used in charging processes. A vessel capable of withstanding a substantial pressure is likely to be constructed with materials and dimensions that give it a fairly large thermal capacitance when compared to that of the entering gas. In the test receiver, for example, the thermal capacitance of the receiver was approximately 8.7 Btu/°R while even at its highest mass the gas capacitance was only of the order of .08 Btu/°R. Thus the gas temperature drop due to heat transfer to the receiver walls would have to be extremely large before any significant change in the wall temperature was observed.

This assumption of no external heat transfer may also be justified by considering the length of time it would take the temperature increase due to heat transfer at the interior surface to reach the outside walls. One method of analyzing this transient conduction heat transfer problem would be to consider the receiver walls a semi-infinite solid with heat transfer

due to convection at the surface. Thus by determining the time (t) required for an observable temperature change to occur in the semi-infinite solid at a distance (x) from the surface equal to the receiver wall thickness of 3/8 inch, some idea of the temperature change at the outside surface of the test tank will be obtained. According to Carslaw and Jaeger [Ref. 4], the solution for this type of problem is given by the equation,

$$\frac{\nu}{V} = \operatorname{erfc}\left(\frac{x}{2\sqrt{\alpha t}}\right) - e^{hx+h^2\alpha t}\operatorname{erfc}\left(\frac{x}{2\sqrt{\alpha t}} + h\sqrt{\alpha t}\right)$$

where

α = the thermal diffusivity of the material

h = h/k = the convective heat transfer coefficient/ the thermal conductivity

ν = the difference between the wall temperature at time t and a distance x from the surface and the initial wall temperature

V = the difference between the gas temperature and the initial wall temperature.

Using the highest value of V recorded throughout our runs (100°R) and a corresponding value for h we find that ν is still only approximately 1.5°R even after 2 minutes have elapsed. Thus for our runs the assumption of no external heat transfer during a charge is justified. This will be the case for all receivers of thermal capacitance sufficient to store the thermal energy, transferred from the gas, with negligible increase in temperature.

E. DISCUSSION OF THE EFFECTS OF IMPERFECT MIXING

In the derivation for determining $\bar{h}$, and in the closed form solutions derived by Reynolds, it was assumed that the effects of imperfect mixing could be neglected. In other words, it was assumed that for analytical purposes the gas can be considered perfectly mixed so that no temperature or pressure gradients exist. As was seen in an unpublished experiment on the heat transfer in a closed container (with similar dimensions to the test receiver) after gas injection [Ref. 5], this is not actually the case. Temperature gradients do exist and this leads to uncertainty in evaluating the heat transfer data correctly. In order to determine the effective temperature potential for heat transfer, use must be made of some sort of average gas temperature so as to keep the complexity of the experimental equipment and the data reduction process reasonable. If this average gas temperature is dependent upon the degree of mixing, then the assumption that the gas is perfectly mixed may lead to erroneous conclusions.

In his paper [Ref. 1], Reynolds showed through the use of a simple comparison between mixed and ummixed gas systems that the pressure is independent of the degree of mixing in an adiabatic receiver regardless of its magnitude. The magnitude of heat transfer in these tests was never very large and, since the average gas temperature used in the derivation for determining h is based directly on the perfect gas law, the temperature thus calculated is fairly independent of the degree of mixing.

Reynolds also showed that the temperature averaged with respect to mass in such an adiabatic receiver was independent of the degree of mixing. Realizing that this average temperature would be very difficult to find experimentally, he went on to compare the temperature averaged with respect to mass and that averaged with respect to volume and found that the discrepancy was so small "that use of a volume average temperature in experimental investigation is entirely satisfactory."[2] Therefore, the average temperature measured by the four thermocouples connected in series at equal volumes vertically in the tank could be used as the temperature referred to as the gas temperature in the closed form solutions.

VI. SUMMARY OF EXPERIMENTAL RESULTS

A. FORM OF RESULTS

The data from a particular run consisted of a pressure and temperature history for the test receiver during charging, and values for the inlet stagnation pressure and temperature. From this data, using the critical flow equation, the mass flow rate for each run was calculated and thus the mass of the gas could be determined for any instant of time. Using this mass and the pressure history of the run, the instantaneous h values were determined by equations (9) and (10). The values of NTU were then calculated and used to determine which class of closed form solution the criteria would designate

---

[2] Reference 1, p. 85.

for this run. The values of $P^* = P/P_0$ as determined by the appropriate closed form solution were then compared with the experimental values. The average percentage deviation between these two values and the average value for NTU throughout a run were then tabulated. Plots were made comparing the P^* values as predicted by Reynolds and those observed experimentally for representative runs. These results are in the form of P^* versus $M^* = M/M_0$ because the pressure readings were slightly more accurate due to the uncertainties involved in determining the temperature of a gas in motion.

The values of h used in determining NTU have been represented by plots of the Nusselt number ($NU = hL/k_f$) versus the product of the Grashof and Prandtl ($GRPR = L^3\rho_f^2 g\beta_f \Delta T/\mu_f^2(c_p\mu/k)_f$) numbers for various runs. The subscript f here indicates that the term was evaluated at the film temperature, which for this case was the mean temperature between that of the gas and the wall. The characteristic length L of the system was taken to be the receiver height for these calculations.

B. HIGH MASS FLOW RATE RUNS

A series of runs was conducted with the test receiver exposed to the ambient atmosphere at high mass flow rates so as to correspond to the adiabatic closed form solution developed by Reynolds. The dimensionless capacitance term $C_0^* = C_c/M_0c_v$, used in the analytical criteria was approximately 657 for all runs. Based on the criteria NTU < .25 for any value of C_0^*, all of these runs were found to correspond

to the so called "adiabatic" case. Values of 1.4 for the ratio of specific heats of the gas (air in this case) and 1.00 for the non-dimensional inlet stagnation term T_1^*, (the inlet stagnation temperature of the gas, T_1 / the original temperature of the gas, T_0) were used in calculating the theoretical P* values from equation (3). Figure 5 is a graphical comparison of the actual and theoretical P* values for representative runs of this type. NU versus GRPR plots for a few typical runs of this nature are seen in figures 11, 12, 13 and 14, the points having been plotted at 1/10 second intervals throughout the runs. Table 2 summarizes the results of this series of tests.

C. LOW MASS FLOW RATE RUNS

A second group of runs was conducted at low mass flow rates so as to correspond to the isothermal closed form solution proposed by Reynolds. Once again, the test receiver was exposed to the surrounding atmospheric conditions. Reynolds' criteria for an isothermal charge solution to hold is NTU > 7 and $C_0^* > 40$. The value of C_0^* for this group of runs was again approximately 657 and the NTU values calculated varied from 1.8 to 14.6. Thus these runs straddle the cutoff value of NTU = 7 and can be used to determine the validity of this figure. The solution for an isothermal charge is simply $P^* = M^*$, for T is a constant and therefore $T^* = 1$. The values of P* predicted by Reynolds and those observed experimentally are compared graphically in figure 6 for representative runs of this type. The h values found in a few

typical runs are presented by the NU versus GRPR graphs of figure 15, 16, 17 and 18. The points in these figures represent 15 second intervals throughout the runs. Table 3 summarizes the results of this series of tests.

D. ISOTHERMAL SINK RUNS

The final group of runs was made, with the test receiver immersed in an ice bath, at intermediate mass flow rates so as to correspond to Reynolds' isothermal sink model. The criteria for this case is simply $C_0^* > 40$. However, in order to avoid crossing into the adiabatic or isothermal solution regions, the value of NTU must be greater than .25 and less than 7 respectively. It should be understood that the ice bath was not necessary in order to meet Reynolds' criteria: with or without it the value of C_0^* (approximately 629 for this case) was large enough to dictate the isothermal sink solution. The ice bath was employed to ensure that the temperature of the receiver walls was a constant and that a significant temperature potential existed between the receiver walls and the gas. Values of 1.4 for the ratio of the specific heats of the gas and 1.00 for the dimensionless inlet temperature, T_1^*, as well as for the dimensionless wall temperature, T_c^*, (the receiver wall temperature T_c/ the original temperature of the gas T_0) were used in calculating the theoretical P* values from equation (5). Figure 7 is a graphical comparison of the actual and theoretical P* values for representative runs of this type. NU versus GRPR plots for a few typical runs of this nature are seen in figure 19, 20 and 21. The points

were determined at 15 second intervals for figure 19, and 1 second intervals for the other two figures. Table 4 summarizes the results of this series of tests.

VII. DISCUSSION OF RESULTS

In order to systematically analyze the test results, the following section is divided into three separate sections. The first section is devoted to an analysis of the equation derived for the convective heat transfer coefficient. The results obtained when comparing the experimentally observed values of P* to those predicted by Reynolds are then discussed. The last section deals with an analysis of the convective heat transfer coefficients obtained with emphasis on the identification of general trends that might be investigated in a more comprehensive study on this topic alone.

A. ANALYSIS OF THE EXPRESSION FOR DETERMINING THE CONVECTIVE HEAT TRANSFER COEFFICIENT EXPERIMENTALLY

In an earlier section the expression

$$h = \frac{-c_v \dot{P}(\frac{V}{R}) + \dot{m}c_p T_i}{A[(\frac{PV}{MR}) - T_w]} \tag{9}$$

was derived with the value for T_w, when it was not considered a constant, given by equation (10).

$$T_w = T_{w_0} + \left(\frac{M_0 c_p}{M_w c}\right)[\frac{M}{M_0}T_i - T] - \left(\frac{c_v V}{RM_w C}\right)[P - P_0] \tag{10}$$

As was mentioned before, these expressions were purposely developed to obtain a value for h from experimentally determined data. Due to the difficulty of measuring the effective average temperature of the gas, this term was eliminated in the above expressions. The equation for h is thus a function of P and M, the other terms being system parameters which were generally held constant and known to a high degree of accuracy throughout a run.

First, considering the expression for the wall temperature, equation (10), it is seen that even when the temperature of the receiver was not held constant the temperature of the walls changed very little during a run. This can be seen by noting the magnitude of the terms in parentheses as well as the fact that the pressure and mass of the gas are never more than one order of magnitude larger than their original conditions (M_0, P_0). An investigation of the values calculated for T_w shows that this was indeed the case for these tests.

Next the expression for the heat transfer coefficient itself will be considered. Since the derivation of this expression was centered about the fact that,

$$h = \frac{q}{A(T-T_w)}$$

it can be seen that the numerator of expression (9) is an expression for the heat transfer q and the denominator is the product of the inside area of the receiver walls and the temperature potential between the walls and the gas. Considering first the denominator, it can be seen that when the temperature of the gas and that of the walls are the same, this term is zero. Of course in this situation, the heat transfer (the numerator of the expression) is also zero and thus as would be expected the convective heat transfer coefficient is undefined. Now, examining the case where there is a finite but small difference between the wall and gas temperatures, as might be the case in a low mass flow rate charging process, it is seen that the equation for h becomes very sensitive to errors in the temperature of the gas or of the receiver walls. It has already been observed that the expression for the temperature of the walls is insensitive to small errors in the values of the system variables, the gas pressure and mass. Unfortunately this is not the case for the perfect gas relation used to express the gas temperature. Even though an error in T may seem negligible when considered on a percentage basis, it is not when considering small differences between T and T_w. For example, an error of 1°R in the temperature of the gas will cut the value for the denominator of h in half

if the temperature difference is only 2°R. A temperature error of this magnitude is definitely within the experimental accuracy of these tests, therefore one must exercise caution when applying this equation to runs in which the temperature potential between the receiver walls and the gas is small.

The numerator of equation (9) can be analyzed in much the same manner. As was the case with the denominator, it can be shown (by examining the normal magnitude of the various terms) that except for the case of small temperature differences this expression is capable of absorbing small errors in P and M without producing a significant error in h.

Combining these results, it is concluded that equation (9) is insensitive to small error in P and M when the temperature difference between the gas and the tank walls is at least of the order of 10°R or greater. Below this value the calculated values of the heat transfer coefficient may be subject to substantial error.

The effect this conclusion has on the confidence in the results of these tests is discussed in the following sections. The actual value of h is used only in the equation for the value of P* in the isothermal sink solution. The runs that correspond to this model have substantial temperature potentials throughout, therefore the values of P* can be calculated with confidence. In the other two cases considered, the values of P* are not a function of the convective heat transfer coefficient, but rather the value of h is used in determining the range of NTU in order to determine the particular solution to be employed. The values of NTU for these runs are dictated

to a greater extent by the mass flow rate than by the convective heat transfer coefficient. For this reason, although the values of NTU may not be exact, they can certainly be used to evaluate the relationship between NTU and the deviation of the theoretical P* values from those actually observed in either of these cases.

The situation is less clear cut when it comes to interpreting the convective heat transfer coefficient data. The sensitivity of the expression for h at low values of the temperature potential places the numerical values for some runs in doubt. The low mass flow rate runs in particular are greatly affected by this uncertainty. For these runs the temperature potential was only on the order of 10°R for the initial runs and decreased as the charging pressure was progressively lowered for each successive set of runs. This does not mean that this data is not meaningful. There is no reason to believe that the trends indicated by such data should not be correct; however, it must be realized that the numerical results are subject to a large range of experimental uncertainty.

B. COMPARISON OF REYNOLDS' MODELS WITH THE EXPERIMENTAL RESULTS

1. High Mass Flow Rate Runs

As was mentioned earlier, all runs of this nature were meant to correspond to Reynolds' adiabatic solution criteria. The value for C_o^* was 657 in all cases and the calculated values of NTU were well below .25 in each run. Reynolds would then recommend that the solution to this type of charging be

approximated by the assumption that there was negligible heat transfer to the receiver walls. When a comparison of the values of the dimensionless pressure as predicted by this solution and those observed experimentally was made the deviation between the two values was of the order of 7.5% of the actual value (see Table 2), with the theoretical value being higher than the actual.

The discrepancy between these two figures may be at least partially accounted for by noting that the assumption that there is no heat transfer is not exact. Since the effect of heat transfer is to lower the change in internal energy of the gas and thus diminish the increase in the gas temperature, a lower gas temperature results with a subsequent reduction in pressure. With this in mind one expects the theoretical P* value to be higher than that actually observed, as is the case for this data.

The parameter NTU is a measure of the thermal conductance (h) relative to the rate of gas flow (w_0). The value of NTU should then be related to the exactness of the assumption of no heat transfer. A connection between NTU and the deviation of the actual and theoretical P* values can be noted in a single run. NTU is directly proportional to h for any particular run, for w_0 is a constant. An increase in h for runs of this sort is accompanied by an increase in the deviation (Fig. 5). Although the quantitative relationship between h and w_0 is not clear from the data for different runs, the increase in h and w_0 is such that their ratio, and hence NTU, increases

with increasing flow. The expected increase in the departure of theory from experiment with increasing NTU is observed in the comparisons (Fig. 8).

Reynolds proposed, on theoretical grounds, that for NTU less than .25 the deviation between actual values of P* and T* and those predicted by the adiabatic solution would be less than 5% for values of M* as high as 9. In the experimental data, this figure seemed valid at the lowest values of NTU ($\approx$.08) recorded and appeared slightly optimistic at higher values (10% deviation at NTU $\approx$.12). In any case, the accuracy of these tests was insufficient to discriminate a 5% deviation and the criteria developed by Reynolds is sufficient for engineering calculations.

In conclusion, it has been seen that the deviation between the actual thermodynamic state of a gas and that predicted by the adiabatic solution for charging is a function of the actual magnitude of the heat transfer in the system. The actual temperature and pressure were always found to be lower than that predicted by the adiabatic solution for the receiver. The parameter NTU proposed by Reynolds seems to be a good measure of whether or not an adiabatic solution should be attempted. His criteria seems satisfactory for all but the most exacting engineering calculations as well. There is also evidence to the fact that the values of the convective heat transfer coefficient and the mass flow rate are not independent in charging processes of this nature.

2. Low Mass Flow Rate Runs

As was discussed in an earlier section, the runs of this type were performed in order to be used in evaluating Reynolds' isothermal model. The value for C_0^* in all cases was 657 and the values of NTU ranged from 1.8 to 14.6. For values of NTU greater than 7, Reynolds recommends the use of the isothermal closed form solution for charging processes. When the values of the dimensionless pressure, P*, as predicted by the isothermal solution and those observed experimentally were compared the deviation between the two values was somewhere between .5% and 4.0% of the actual value (see Table 3). In all cases this deviation proved to be negative; that is, the actual pressure and temperature were higher than those predicted in an isothermal solution to the charging process.

The deviation in the isothermal values of P* and the actual values for these runs were small and can be accounted for by investigating the assumptions that lead to the isothermal charging model. In this model the thermal capacitance of the receiver was assumed infinite while the internal heat transfer resistance was taken to be zero. Therefore, any tendency for the incoming gas to heat up was countered by an immediate transfer of heat to the receiver walls. This condition was approached by charging so slowly that the gas and the walls, initially at the same temperature, remained at that state. This model can not be exact since the interfaces between the gas and the walls have a finite heat transfer resistance, thus the resulting discrepancies between the actual and theoretical values for P*.

It seems reasonable to predict in view of the preceding discussion that an increase in the heat transfer resistance (a decrease in h) would lead to an increased deviation in the isothermal and actual values for P^*. Although the values for h were subject to error in these runs (see section VII-A), a definite downward trend throughout a single run was noted (Fig. 15, 16, 17 and 18). As predicted, this decrease in h was accompanied by an increase in the deviation of the P^* values (Fig. 6).

An examination of the effect of NTU on the deviation of the isothermal and actual thermodynamic state of the gas was then made. It was noted that the values of h for different runs remained constant within experimental scatter regardless of the value of w_0. Thus, unlike the adiabatic case where the effects of changing w_0 seemed to be offset by corresponding changes in h, the value of NTU for this type of charging was inversely proportional to the value of w_0. Once again NTU proved to be a good measure of the deviation, for as w_0 decreased the percentage deviation decreased (Fig. 9).

The criteria proposed by Reynolds suggests that for values of NTU larger than 7 an isothermal solution for a charging process will give less than 5% deviation from the actual thermodynamic state of the gas. The data from these tests indicates that for values of NTU as low as 2 the deviation is still less than 5%, therefore it seems that Reynolds' criteria is slightly conservative. Of course, it must be pointed out that the value of C_0^* for these runs was 657 and this is well

above the value of $C_0^* > 40$ listed along with the NTU > 7 criteria. Nonetheless, it can safely be asserted that for values of C_0^* above 40 and values of NTU of 7 or greater, the isothermal solution to a charging process will give good accuracy.

In conclusion, it was observed that the actual temperature and pressure in a receiver being charged are consistently higher than those predicted by an isothermal solution. The parameter proposed by Reynolds once again appeared to be a good indicator as to whether or not an assumption of isothermal charging can be applied to a particular process. Reynolds' criteria also proved to be very satisfactory for engineering purposes. Finally, evidence was observed that the value of the convective heat transfer coefficient and the mass flow rate can be considered independent in a charging process of this nature.

3. Isothermal Sink Runs

The last group of runs to be evaluated were those made with the test receiver immersed in an ice bath. These runs were performed at intermediate values of NTU so as to correspond to Reynolds' isothermal sink closed form solution. The only criterion specified for the use of this method is that the dimensionless capacitance term be greater than 40. In all the runs of this nature the value for C_0^* was 626, therefore this criteria was easily satisfied. Of course, Reynolds implies that the value of NTU dictating an isothermal sink solution (to approximate the actual conditions) be between .25 and 7, for if not the regions encountered prescribe either the

adiabatic or the isothermal solution. When the values of the dimensionless pressure as predicted by the isothermal sink solution and those observed experimentally were compared, the deviation between the two values was somewhere between 8% and 14.5% of the experimental value.

It should be noted here that the isothermal sink solution is an intermediate case between the two extremes of an adiabatic solution and the isothermal solution. Therefore, the thermodynamic state of the gas must be expressed as a function of the heat transfer coefficient and the mass flow rate in the closed form solution (see equations (4) and (5)).

As before, physical interpretations were sought for the deviation between the isothermal sink solution for the thermodynamic state of the gas and that actually observed. The assumption on which this model was built was that the temperature of the thermal capacitance remained a constant even after absorbing the energy released by the gas in the receiver. If the comparatively small amounts of heat transferred to the receiver walls were uniformly distributed throughout the very large thermal capacitance, this assumption might be quite accurate. However, as was seen by an investigation using the heat conduction equation for a semi-infinite solid (see section V-D) most of the internal energy (as indicated by the temperature distribution) never gets any farther than the first few tenths of an inch in a charging process of this nature. For this reason the temperature at the wall surface does not remain constant but rather increases slightly even

though the effective thermal capacitance of the receiver is still extremely large. Bearing this in mind, the actual temperature potential between the inside surface of the receiver walls and the gas is overestimated by the isothermal sink solution. Therefore, the amount of heat transferred out of the gas and the accompanying temperature and pressure drops are slightly exaggerated in this closed form solution (Fig. 7).

To begin an evaluation of the parameters that affect the deviation between theory and experiment, single runs, in which the mass flow rates were constant, were examined. For the low mass flow runs there seemed to be only a very gradual increase in the value of h as the run proceeds. At higher values of the flow rate the increases in h during a run were more substantial as were their magnitudes (Figs. 19-21). Using both the low mass flow runs (almost constant h) and the high flow rate runs (increasing h) it was possible to examine the effect of h on the deviation between an actual run and the thermodynamic state predicted for this run by the isothermal sink solution. In analyzing the data (Figs. 7 and 10) the conclusion was reached that the deviation was apparently not closely dependent on the value of h. In both the low flow rate runs and the high flow rate runs the deviation followed the same pattern throughout a run and likewise there was no discernible connection between the magnitude of the deviation and the values for h. In any case it is probable that the effect, if any, of the value of h on the deviation

of experimental and isothermal sink values is masked by the use of NTU = hA/w_0c_v as a parameter in equations (4) and (5).

For the two extreme solutions (adiabatic and isothermal) presented in the previous sections, their accuracy increased as the appropriate extreme condition was approached. This might lead one to believe that the intermediate ranges of NTU for the isothermal sink solution now being considered would most closely correlate to the actual thermodynamic state of the gas during charging. Since the data does not cover the entire range of NTU between .25 and 7, no conclusive statement can be made in this regard. Figure 10, however, supports the notion that as NTU approaches an intermediate value of say 3.5 the deviation decreases. One thing can be asserted, and that is that, due to the connection between w_0 and h in this type of charging, the values of NTU do not vary greatly. Thus, regardless of the connection between NTU and the deviation, it seems certain that the deviation between the isothermal sink solution and that actually observed is approximately constant for a particular system as long as the flow rates are of the same order of magnitude.

In conclusion, it should be noted that the isothermal sink closed form solution is a function of the convective heat transfer coefficient and the mass flow rate, and thus differs from the previous two closed form solutions. The deviation between the thermodynamic state of the gas as predicted by the analytical solution and that observed experimentally was between 8% and 15% of the experimental value. The closed form solution values were consistently lower than

those found in the tests. This discrepancy can be explained by the fact that the predicted value of the temperature of the thermal capacitance in Reynolds' solution is lower than that actually existing. The heat transfer and temperature drop are subsequently overestimated in this solution. For runs of this nature it was also observed that the values of h increase throughout a run and that not only the magnitude of this increase but the values of h are increased when the mass flow rate is increased. There seemed to be little or no dependence of the accuracy of the isothermal sink assumption on the values for h when w_0 is a constant. No conclusive statement can be made as to the connection between NTU and the deviation of the isothermal sink solution and the actual values, although there is evidence to support a prediction that this solution is most accurate at intermediate values of NTU. Due to the apparent connection between w_0 and h the values of NTU do not change substantially for runs in this region nor do the percentage deviation in the values for the thermodynamic state of the gas. Lastly, for this particular experiment the discrepancy between the solution as predicted by an isothermal sink solution and that observed experimentally, was slightly higher than that predicted by Reynolds even though the value of C_0^* was well above the criteria value of 40.

C. DISCUSSION OF THE EXPERIMENTALLY OBTAINED HEAT TRANSFER COEFFICIENTS

Having empirically obtained values for the convective heat transfer coefficient throughout the various runs, an attempt was made to obtain at least a qualitative explanation of the behavior of these values. The charging situation was substantially different from those usually described in convection theories. The pressure of the system is usually not varied in such theories, nor is the direction and magnitude of the flow velocity a function of variables other than position. Since any attempt to arrive at a theoretical expression for the convective heat transfer coefficient in a receiver being charged would be completely beyond the scope of this paper, no attempt was made. Some insight was gained, however, in considering the possible non-dimensional parameters that might affect an expression for the convective heat transfer in a charging situation.

From the general equations of motion and energy, an average convective heat transfer coefficient evaluated over the total surface area of a body (this eliminates any spatial dependence) can be expressed as a function of the dimensionless parameters as listed below:

$$NU = hL/k = f(PR,\ ER,\ GR,\ RE) \quad .$$

An investigation of these parameters was then made in order to come to a better understanding of the causes for the behavior of h in the experimental data. First to be considered was the Prandtl number. Defined as

$$PR = \mu c_p/k$$

this dimensionless number can be considered constant and of the order of 1 for solutions involving perfect gases. Having concluded that the effects of the Prandtl number need not be considered, the Eckert number was then considered. This non-dimensional parameter expresses the ratio of the inertia terms to the enthalpy terms and is defined as

$$ER = U^2/c_p\Delta T$$

where U is the characteristic velocity of the flow and $c_p\Delta T$ is the change in enthalpy across the boundary layer. In the charging processes carried out for this paper the average gas velocities were small as compared to the enthalpy, therefore the effect of the Eckert number is considered negligible.

As has been pointed out, a common practice is to take the Grashof number as the governing parameter for the heat transfer processes of the kind under consideration here. Defined as,

$$GR = gL^3\beta\Delta T\rho^2/\mu^2$$

this term is the ratio of the buoyancy to the viscous effects. The buoyancy of the fluid aids the heat transfer by supporting the motion of the fluid at the surface of the receiver walls. Noting this, the Grashof number must be considered significant in determining the convective heat transfer coefficient in a charging process of the sort presented here. Since considerable motion is also present in the tank due to the stirring action of the injection, the Reynolds number, defined as

$$RE = U\rho\ell/\mu$$

must also be considered. In the above expression, U is again a characteristic velocity of the flow and ℓ a characteristic length for the flow. This dimensionless number can be seen to be a measure of the relative importance of the inertia and viscous effects and often occurs in the analysis of problems in forced convection.

Investigating the variables comprising these non-dimensional parameters leads to some understanding as to their magnitude and behavior for charging processes. For small temperature changes the density can be considered proportional to the pressure. If the temperature changes are significant the density is both proportional to the pressure and inversely proportional to the temperature. The viscosity is almost independent of pressure and increases slightly with temperature. For situations of an isothermal nature, it is then expected that the variables in the Reynolds number are the velocity, the density (which is proportional to the pressure) and perhaps, the characteristic length of the fluid flow. If the temperature changes throughout a process are large, once again the Reynolds number is proportional to the velocity, the density (now proportional to the pressure and inversely proportional to the temperature), the characteristic length, and also inversely proportional to the viscosity (which is proportional to the temperature). Now applying the same sort of reasoning to the Grashof number, the effect of μ as a variable in a moderate temperature change system can again be eliminated along with the gravitational constant, g. The density behaves

in the manner described in the Reynolds number discussion. The coefficient of volumetric expansion, β, is defined as

$$\beta = -\frac{1}{\rho}\left(\frac{\partial\rho}{\partial T}\right)_P$$

and varies as the inverse of the temperature for a perfect gas. The term ΔT in the Grashof number is the temperature change across the boundary layer and L is the characteristic length of the system, a constant.

In preparation for applying what was learned about the factors affecting the heat transfer coefficient to the behavior observed in the experimental runs, the velocity variations in the test receiver were examined. When the inlet valve for the receiver was first opened a pressure ratio (the receiver back pressure/ the stagnation pressure upstream of the flow meter) considerably smaller than the critical pressure ratio existed across the flow metering device. Sonic flow was established at the throat of the inlet to the tank. Therefore, fluid entering at a pressure corresponding to the sonic conditions was forced to adjust to the lower back pressure in the tank. Regardless of the form of this adjustment it must have been coupled to a substantial increase in the local velocity. As the back pressure in the receiver increased, the pressure adjustment became less severe and thus the local velocity decreased throughout a charging process. Here the term "local" applies to the conditions in the tank near the point of injection.

For the low mass flow rate runs the temperature potential between the gas and the walls, ΔT, was very small. For this

reason it was felt that the Grashof number was not as significant as the Reynolds number throughout these runs. Having seen that during a charge the velocity near the injector decreased, it was thought that perhaps the characteristic length over which the incoming jet acts was also decreased. Therefore, although the density increased due to the increase in pressure, it seemed reasonable to assume that the Reynolds number decreased slightly throughout a run. A drop in the Nusselt number, and thus the convective heat transfer coefficient, was predicted. In other words, forced convection gives way to free convection as the run slowly proceeds. Figures 15, 16, 17 and 18 seem to support a conclusion of this sort. This notion also is supported in a paper by Ulrich et. al. [Ref. 6] in which the mode of heat transfer following gas injection was observed to proceed from forced to free convection. For the high mass flow rate and isothermal sink runs, the temperature potential was much greater than that for the low mass flow rate runs, thus the Grashof number was expected to be more significant in these processes. Since the Grashof number is greatly affected by a pressure increase as dictated by the ρ^2 term, it was felt that the Nusselt number would increase throughout a run. Once again these assumptions seem to be supported by the data, see figures 11, 12, 13 and 14 as well as 19, 20 and 21.

As to the actual magnitude of the convective heat transfer coefficient as indicated by NTU, the data was hard to correlate. As seemed consistent with the conclusions drawn above, the values of the Nusselt and Grashof numbers for the low mass

flow rate runs were lower than those for the high mass flow rate and isothermal sink cases. However, with the exception of the set of runs at a very low mass flow rate (perhaps corresponding to the low ΔT discussion above), the isothermal sink values were above those for the high mass flow rate runs. One possible explanation for this was the fact that the isothermal sink runs were recorded in 1 second intervals for run times of 7 to 9 seconds. The high mass flow rate runs, on the other hand, were only of 1 second duration with the points measured at 1/10 second intervals. Therefore it might be that for runs of larger duration, the mixing motion caused by the impinging jet could spread more thoroughly throughout the receiver. These types of forced convection phenomena could not be adequately described on the basis of the results of these tests. In any case, the values calculated in these tests are at most 1 order of magnitude above those predicted by free convection theories (Figs. 11-21). Therefore if no better estimate of the heat transfer coefficient can be obtained, a value based on these theories could be used for processes of the nature discussed here.

The preceding discussion was based mainly on physical intuition and is only crudely substantiated by the few experimental runs performed in this undertaking. As will be repeated in the recommendations, a much more extensive and controlled study is needed in this area to draw any conclusive relationships between the convective heat transfer coefficient and the many variables in a system being charged.

VIII. CONCLUSIONS

The general conclusions to be drawn from this investigation are summarized as follows.

(a) Excellent quantitative agreement between the experimental values and those predicted by Reynolds [Ref. 1] has been obtained for the thermodynamic state of a gas in a receiver being charged.

(b) The parameter NTU prescribed by Reynolds is a good indicator for describing the extent of heat transfer in a receiver being charged.

(c) The technique developed in this paper for experimentally determining the convective heat transfer coefficient may be confidently used in conjunction with Reynolds' closed form solutions if the temperature potential between the receiver walls and the charging gas is of an order of 10°R or larger.

(d) The convective heat transfer coefficient is related to the initial mass flow rate of the entering gas for all but the extremely slow charging rates (w_0 < .003 lbm/sec.).

(e) The heat transfer coefficient for charging of the nature described in this paper can be estimated within one order of magnitude by free convection theories. The heat transfer coefficient thus obtained will be equal to or less than the actual value. The effects of errors in this estimate

will be small provided that the NTU is sufficiently small (high injection rates).

IX. RECOMMENDATIONS

(1) It is recommended that an extensive and controlled study of the effects of the various system parameters on the convective heat transfer coefficient during charging be made with emphasis placed on the development of an empirical formula for use in this area.

(2) A possible extension of the technique for experimentally determining the convective heat transfer coefficient developed in this paper could include the use of analog computer methods to directly analyze the pressure and temperature signals from probes in the vessel.

(3) In any further investigation of the type discussed in this paper, the following suggestions are made. A more exact method of measuring the mass flow rate should be developed. Care should also be taken to eliminate any possible transient effects in establishing flows used in experiments of this nature. It is also recommended that hot gases be used in order to obtain substantial temperature potentials between the receiver walls and the gas.

APPENDIX A

Nomenclature of Reference 1

English Letter Symbols

A	Area, ft^2
C_c	Thermal Capacitance of receiver shell, Btu/°R
c_p	Specific heat at constant pressure, Btu/(lb°R)
c_v	Specific heat at constant volume, Btu/(lb°R)
h	Specific enthalpy, Btu/lb
h	Unit heat transfer convective conductance, Btu/(hr ft^2°R)
k	Thermal conductivity, Btu/(hr ft^2°R/ft)
M	Mass, lb
P	Pressure, lb/ft^2
q	Heat transfer rate, Btu/hr
T	Absolute temperature, °R
U	Total internal energy, Btu
u	Specific internal energy, Btu/lb
V	Volume, ft^3
w	Mass flow rate, lb/hr

Greek Letter Symbols

θ	Time, hr
μ	Viscosity, lb/(hr ft)
ρ	Density, lb/ft^3
Δ	Denotes a difference

Nondimensional Grouping

C_0^*	$C_c/(M_0 c_v)$
k	c_p/c_v
M^*	M/M_0
NTU	$1/(R_i c_v w_0) = (hA)_i/c_v w_0$
NTU_∞	$1/(R_\infty c_v w_0) = (hA)_\infty/c_v w_0$
P^*	P/P_0
T^*	T/T_0
T_1^*	T_1/T_0
T_c^*	T_c/T_0
T_∞^*	T_∞/T_0
w^*	w/w_0

Subscripts

0	Refers to initial conditions
1	Refers to inlet state
c	Refers to capacitance
i	Refers to inside receiver
∞	Refers to environmental conditions outside receiver

APPENDIX B

Derivation of General Differential Equation and Closed Form Solutions for Charging

Assumptions and Idealizations

(1) The walls of the receiver are at a uniform temperature throughout.

(2) The heat transfer resistances both inside and outside are constant and uniform throughout their respective surface areas.

(3) Perfect mixing of the injected gas and the gas in the receiver.

(4) The working fluid is a thermally and calorifically perfect gas.

(5) The specific heat of the capacitance is a constant.

(6) The kinetic energy of the gas in the receiver may be neglected.

General Differential Equation for Charging

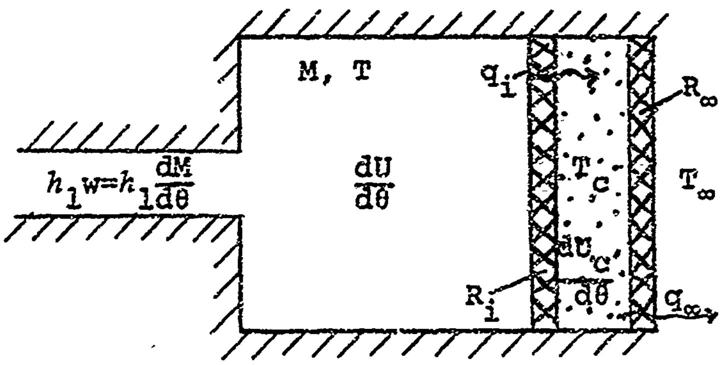

An energy balance on the receiver, using h_1 as the stagnation enthalpy of the inlet gas gives,

$$h_1 \frac{dM}{d\theta} = \frac{dU}{d\theta} + q_i \ .$$

An energy balance on the receiver walls yields,

$$q_i = \frac{dU_c}{d\theta} + q_\infty \ .$$

The heat transfer rates can be defined in terms of the temperature potential and the heat transfer resistance as follows:

$$q_i = \frac{T-T_c}{R_i} , \quad q_\infty = \frac{T_c-T_\infty}{R_\infty} .$$

The change in the total internal energy of the gas in the receiver may be written in terms of the mass and the specific internal energy as,

$$\frac{dU}{d\theta} = M\frac{du}{d\theta} + u\frac{dM}{d\theta} \ .$$

The rate of change of energy in the capacitance may be expressed as,

$$\frac{dU_c}{d\theta} = \frac{d(C_cT_c)}{d\theta} = C_c\frac{dT_c}{d\theta} \ .$$

Thus, the energy balance on the gas may be written as,

$$h_1 \frac{dM}{d\theta} = M\frac{du}{d\theta} + u\frac{dM}{d\theta} + \frac{T-T_c}{R_i}$$

or

$$(h_1-u)\frac{dM}{d\theta} = M\frac{d(c_vT)}{d\theta} + \frac{T-T_c}{R_i}$$

and thus,

$$(c_pT_1-c_vT)\frac{dM}{d\theta} = c_vM\frac{dT}{d\theta} + \frac{T-T_c}{R_i} \ .$$

Note here that T_1 is the stagnation temperature of the inlet gas. Therefore, dividing by c_v gives,

$$(kT_1 - T)\frac{dM}{d\theta} = M\frac{dT}{d\theta} + \frac{T-T_c}{R_i} \quad .$$

In a similar fashion the energy balance on the capacitance can be written as,

$$\frac{T-T_c}{R_i} = C_c \frac{dT_c}{d\theta} + \frac{T_c - T_\infty}{R_\infty}$$

then dividing by C_c,

$$\frac{dT_c}{d\theta} = \frac{T-T_c}{R_i C_c} - \frac{T_c - T_\infty}{R_\infty C_c} \quad .$$

Therefore,

$$\frac{dT_c}{d\theta} = \frac{T}{R_i C_c} + \frac{T_\infty}{R_\infty C_c} - \frac{T_c}{C_c}\left(\frac{1}{R_i} + \frac{1}{R_\infty}\right) ,$$

The instantaneous mass flow rate, w, may be defined as

$$w = \frac{dM}{d\theta}$$

and we can write,

$$\frac{dT}{d\theta} = \frac{dT}{dM}\frac{dM}{d\theta} = w\frac{dT}{dM}$$

as well as,

$$\frac{dT_c}{d\theta} = \frac{dT_c}{dM}\frac{dM}{d\theta} = w\frac{dT_c}{dM} \quad .$$

The equation for the energy of the gas may then be written as,

$$(kT_1 - T)w = wM\frac{dT}{dM} + \frac{T-T_c}{R_i c_v}$$

or

$$wM\frac{dT}{dM} + \frac{T-T_c}{R_i c_v} + (T-kT_1)w = 0 \quad . \qquad (1)$$

In a similar manner the energy equation of the capacitance can be written as

$$w\frac{dT_c}{dM} = \frac{T}{R_iC_c} + \frac{T_\infty}{R_\infty C_c} - \frac{T_c}{C_c}(\frac{1}{R_i} + \frac{1}{R_\infty})$$

or

$$w\frac{dT_c}{dM} + \frac{T_c}{C_c}(\frac{1}{R_i} + \frac{1}{R_\infty}) - \frac{T}{R_iC_c} - \frac{T_\infty}{R_\infty C_c} = 0. \qquad (2)$$

Expressing equation (1) in dimensionless form by dividing through by T_0 and noting that

$$M\frac{d}{dM} = \frac{M}{M_0}\frac{d}{d(\frac{M}{M_0})} = M^*\frac{d}{dM^*}$$

we obtain,

$$wM^*\frac{dT^*}{dM^*} + \frac{T^*-T_c^*}{R_ic_v} + (T^*-kT_i^*)w = 0 .$$

Now dividing by w_0 and noting the definition of NTU, we obtain the dimensionless form,

$$w^*M^*\frac{dT^*}{dM^*} + (T^*-T_c^*)NTU + (T^*-kT_i^*)w^* = 0 . \qquad (1a)$$

In the same way, equation (2) can be non-dimensionalized by dividing through by T_0w_0/M_0 so that,

$$w^*\frac{dT_c^*}{dM^*} + \frac{T_c^*M_0}{C_cw_0}(\frac{1}{R_i} + \frac{1}{R_\infty}) + \frac{T^*M_0}{R_iw_0C_c} - \frac{T_\infty^*M_0}{R_\infty C_cw_0} = 0$$

and noting that NTU/C_0^* is equal to $M_0/R_iw_0C_c$ the following is obtained,

$$w^*\frac{dT_c^*}{dM^*} + T_c^*(NTU+NTU_\infty) - \frac{NTU}{C_0^*}T^* - \frac{NTU_\infty}{C_0^*}T_\infty^* = 0 . \qquad (2a)$$

These two dimensionless equations can be combined to yield a single equation giving T^* as a function of M^* by differentiation

of equation (1a) with respect to M* and suitable arithmetic manipulations represented below:

$$w^*M^*\frac{dT^*}{dM^*} + (T^*-T_c^*)NTU + (T^*-kT_1^*)w^* = 0 \quad . \qquad (1a)$$

Differentiation with respect to M* yields,

$$\frac{dw^*}{dM^*}(M^* + \frac{dT^*}{dM^*}) + w^*(\frac{dT^*}{dM^*} + M^*\frac{d^2T^*}{dM^{*2}}) + (\frac{dT^*}{dM^*} - \frac{dT_c^*}{dM^*})NTU$$

$$+ w^*(\frac{dT^*}{dM^*}) + (\frac{dw^*}{dM^*})T^* - kT_1^*(\frac{dw^*}{dM^*}) = 0$$

rearranging the following is obtained,

$$\frac{dT_c^*}{dM^*} = \frac{w^*(2\frac{dT^*}{dM^*} + m^*\frac{d^2T^*}{dM^{*2}})}{NTU} + \frac{dT^*}{dM^*}$$

$$+ \frac{\frac{dw^*}{dM^*}(T^*+M^*\frac{dT^*}{dM^*})}{NTU} - \frac{w^*kT_1^*\frac{dw^*}{dM^*}}{NTU} \quad .$$

Substituting this expression for dT_c^*/dM^* in equation (2a),

$$\frac{w^{*2}m^*\frac{d^2T^*}{dM^{*2}}}{NTU} + \frac{2w^{*2}\frac{dT^*}{dM^*}}{NTU} + w^*\frac{dT^*}{dM^*} + \frac{w^*\frac{dw^*}{dM^*}(T^*+M^*\frac{dT^*}{dM^*})}{NTU}$$

$$- \frac{w^*kT_1^*\frac{dw^*}{dM^*}}{NTU} + \frac{T_c^*}{C_0^*}(NTU+NTU_\infty) - \frac{NTU}{C_0^*}T^* - \frac{NTU_\infty}{C_0^*}T_\infty^* = 0 \quad .$$

Multiplying through by NTU and combining gives,

$$w^*M^*\frac{d^2T^*}{dM^{*2}} + w^*(2w^*+NTU+M^*\frac{dw^*}{dM^*})\frac{dT^*}{dM^*}$$

$$+ (w^*\frac{dw^*}{dM^*} - \frac{NTU^2}{C_0^*})T^* - \frac{NTU_\infty NTU}{C_0^*}T_\infty^* - w^*kT_1^*\frac{dw^*}{dM^*} \qquad (3)$$

$$+ \frac{T_c^*}{C_0^*}(NTU+NTU_\infty)NTU = 0 \quad .$$

Now solving (1a) for T_c^*,

$$T_c^* = \frac{w^*M^*\frac{dT^*}{dM^*} + T^*NTU+T^*w^*-kT_1^*w^*}{NTU} .$$

Therefore the term,

$$\frac{T_c^*}{C_0^*}(NTU+NTU_\infty)NTU$$

in the above expression can be written as,

$$w^*M^*\frac{dT^*}{dM^*}\left(\frac{NTU+NTU_\infty}{C_0^*}\right) + \frac{T^*NTU}{C_0^*}(NTU+NTU_\infty)$$

$$+ \frac{w^*T^*}{C_0^*}(NTU+NTU_\infty) - \frac{kT_1^*w^*}{C_0^*}(NTU+NTU_\infty) .$$

Substituting this in equation (3) we arrive at the general differential equation for charging.

$$w^*M^*\frac{d^2T^*}{dM^{*2}} + w^*\left[2w^*+NTU+M^*\frac{dw^*}{dM^*} + \left(\frac{NTU+NTU_\infty}{C_0^*}\right)M^*\right]\frac{dT^*}{dM^*}$$

$$+ \left[w^*\frac{dw^*}{dM^*} + \frac{1}{C_0^*}(NTU+NTU_\infty)w^* + \frac{NTU\ NTU_\infty}{C_0^*}\right]T^*$$

$$- kT_1^*w^*\frac{dw^*}{dM^*} - \frac{NTU+NTU_\infty}{C_0^*}w^*kT_1^* - \frac{NTU\ NTU_\infty}{C_0^*}T_\infty^* = 0 .$$

<u>Closed Form Solution for Adiabatic Charging</u>

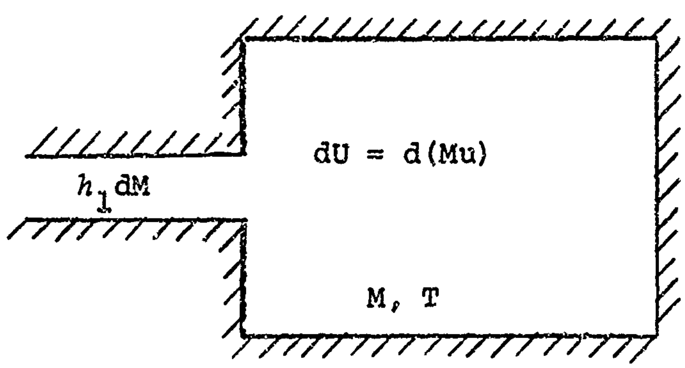

Since there are no heat transfer rates to consider in an adiabatic solution it is not necessary to specify the mass flow rate. An energy balance on the gas in the receiver, using stagnation functions, gives

$$h_1 dM = d(mu) = Mdu + udM$$

or

$$(h_1 - u)\,dM = Mdu \quad .$$

Then one can write,

$$(c_p T_1 - c_v T)\,dM = Mc_v dT \quad .$$

Dividing by c_v gives,

$$(kT_1 - T)\,dM = Mdt \quad .$$

In order to get this equation in dimensionless form, we divide through by $T_0 M_0$, thus obtaining

$$(kT_1 - T^*)\,dM^* = M^* dT^* \quad .$$

Now separating variables and integrating this equation from the initial conditions ($T = T_0$, $M = M_0$) to a state at a later time ($T = T$, $M = M$),

$$\int_{\frac{T_0}{T_0}}^{\frac{T}{T_0}} \frac{dT^*}{(kT_1^* - T^*)} = \int_{\frac{M_0}{M_0}}^{\frac{M}{M_0}} \frac{dM^*}{M^*} \quad .$$

This gives,

$$-\log(k_1 T_1^* - T^*) + \log(kT_1^* - 1) = \log M^* \quad .$$

Rearranging, this equation reduces to

$$\frac{(kT_1^* - 1)}{M^*} = kT_1^* - T^* \quad .$$

Solving for T*, the final result is obtained,

$$T^* = kT_1^* - \frac{(kT_1^*-1)}{M^*} \quad .$$

Thus having derived a relation for T* as a function of M*, the perfect gas relation $P^* = M^*T^*$ is used to obtain,

$$P^* = kT_1^*(M^*-1) + 1 \quad .$$

<u>Closed Form Solution for Isothermal Charging</u>

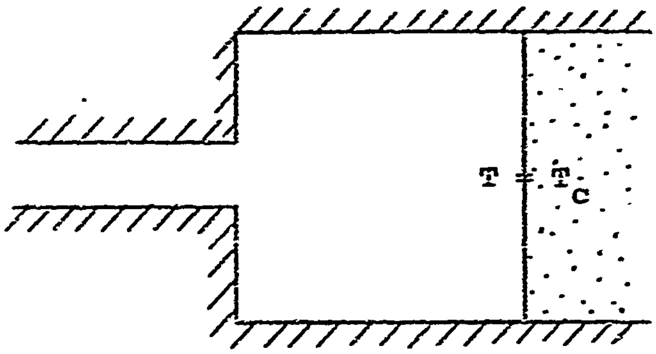

Since T = constant = $T_0 = T_c$, then

$$T^* = \frac{T}{T_0} = 1 \quad .$$

Therefore the isothermal pressure mass relationship can be obtained directly from the perfect gas law, and is

$$P^* = M^* \quad .$$

Closed Form Solutions for Charging at Constant Mass Flow with Heat Transfer to an Isothermal Sink

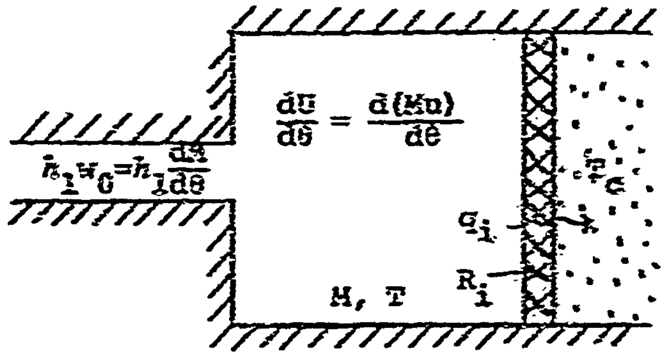

An energy balance on the gas using stagnation functions gives,

$$\bar{h}_1\frac{dM}{d\theta} = q_i + \frac{d(Mu)}{d\theta} = q_i + u\frac{dM}{d\theta} + \frac{du}{d\theta}M \quad .$$

By definition of the heat transfer resistance R_i,

$$q_i = \frac{T-T_c}{R_i}$$

and using $w = dM/d\theta$, then

$$c_pT_1w_0 = \frac{T-T_c}{R_i} + M\frac{du}{d\theta} + w_0c_vT$$

or

$$c_pT_1w_0 = \frac{T-T_c}{R_i} + Mc_v\frac{dT}{d\theta} + w_0c_vT \quad .$$

Using the following relation,

$$\frac{dT}{d\theta} = \frac{dT}{dM}\,\frac{dM}{d\theta} = w_0\frac{dT}{dM}$$

and dividing by w_0 and rearranging the expression becomes,

$$-c_pT_1 + c_vM\frac{dT}{dM} + c_vT + \frac{T-T_c}{R_iw_0} = 0 \quad .$$

Now dividing by c_v to obtain

$$M\frac{dT}{dM} + T - kT_1 + \frac{T-T_c}{R_i W_0 c_v} = 0 \quad .$$

Note that all functions refer to stagnation conditions. In order to get this equation in dimensionless form it is divided by T_0 so that,

$$\frac{M}{T_0}\frac{dT}{dM} + T^* - kT_1^* + (T^*-T_c^*)\frac{1}{R_i W_0 c_v} \quad .$$

Since

$$\frac{M}{T_0}\frac{dT}{dM} = \frac{M}{M_0}\frac{d(\frac{T}{T_0})}{d(\frac{M}{M_0})} = M^*\frac{dT^*}{dM^*} \text{ and } NTU = \frac{1}{R_i W_0 c_v}$$

this expression can be written as,

$$M^*\frac{dT^*}{dM^*} + (T^*-kT_1^*) + (T^*-T_c^*)NTU = 0 \quad .$$

In order to obtain the closed form solution the variables are separated and the expression integrated from the initial conditions ($T = T_0$, $M = M_0$) to a state at a later time ($T = T$, $M = M$).

$$\int_{\frac{T_0}{T_0}}^{\frac{T}{T_0}} \frac{dT^*}{[T^*(1+NTU)-kT_1^*-NTUT_c^*]} = -\int_{\frac{M_0}{M_0}}^{\frac{M}{M_0}} \frac{dM^*}{M^*} \quad .$$

This gives

$$\frac{1}{(1+NTU)}\log[-kT_1^*-NTUT_c^*+(1+NTU)T^*]$$

$$-\frac{1}{(1+NTU)}\log[-kT_1^*-NTUT_c^*+(1+NTU)] = -\log M^*$$

or

$$-kT_1^* - NTUT_c^* + (1+NTU)T^* = M^{*-(1+NTU)}[-kT_1-NTUT_c^*+(1+NTU)] \ .$$

Solving this expression for T* as a function of M* the following is obtained:

$$T^* = \frac{kT_1^*+NTUT_c^*-(kT_1^*+NTUT_c^*-1-NTU)M^{*-(1+NTU)}}{(1+NTU)} \ .$$

Using the perfect gas law,

$$p^* = \frac{(kT_1^*+NTUT_c^*)M^*-(kT_1^*-1-NTU+NTUT_c^*)M^{*-NTU}}{1+NTU}$$

<u>Closed Form Solution for Charging at Constant Mass Flow with Inside Resistance Negligible</u>

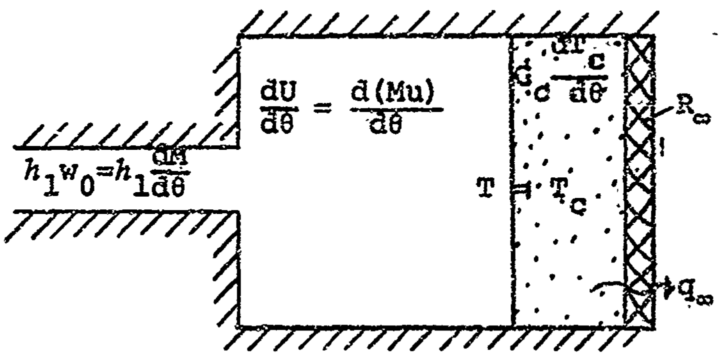

An energy balance on the gas and the capacitance combined yields,

$$h_1\frac{dM}{d\theta} = \frac{d(Mu)}{d\theta} + C_c\frac{dT_c}{d\theta} + q_\infty \ .$$

By definition of the heat transfer resistance between the capacitance and the surrounding medium, R_∞,

$$q_\infty = \frac{T_c-T_\infty}{R_\infty} = \frac{T-T_\infty}{R_\infty} \ .$$

Now since $w_0 = dM/d\theta$ the expression

$$\frac{dT}{d\theta} = \frac{dT}{dM}\frac{dM}{d\theta} = w_0\frac{dT}{dM}$$

can be written. Using this expression and the perfect gas relationships in the original energy balance,

$$-c_pT_1\frac{dM}{d\theta} + \frac{dM}{d\theta}c_vT + Mc_v\frac{dT}{d\theta} + C_c\frac{dT}{d\theta} + \frac{T-T_\infty}{R_\infty} = 0 \quad .$$

Dividing through by $c_v dM/d\theta$ or $c_v w_0$ and noting that $dT_c/d\theta = dT/d\theta$,

$$-kT_1 + T + (M+\frac{C_c}{c_v})\frac{dT}{dM} + \frac{T-T_\infty}{c_vR_\infty w_0} = 0 \quad .$$

In order to express this equation in terms of non-dimensional temperature, T^*, it is divided by T_0 to obtain,

$$M^*\frac{dT^*}{dM^*} + C_0^*\frac{dT^*}{dM^*} - kT_1^* + T^*(T^*-T_\infty^*)NTU_\infty = 0 \quad .$$

The variables are now separated and the expression integrated from the initial conditions ($T = T_0$, $M = M_0$) to a state at a later time ($T = T$, $M = M$).

$$\int_{\frac{T_0}{T_0}}^{\frac{T}{T_0}} \frac{dT^*}{T^*(1+NTU_\infty)-kT_1^*-NTU_\infty T_\infty^*} = \int_{\frac{M_0}{M_0}}^{\frac{M}{M_0}} \frac{dM^*}{M^*+C_0^*} \quad .$$

The solution to the above gives,

$$\log[T^*(1+NTU_\infty)-kT_1^*-NTUT_\infty^*] = -(1+NTU_\infty)\log\frac{(M^*+C_0^*)}{(1+C_0^*)}$$

$$+ \log[-kT_1^*-NTU_\infty T_\infty^*+(1+NTU_\infty)]$$

or

$$T^*(1+NTU_\infty) - kT_1^* - NTU_\infty T_\infty^*$$

$$= \left[\frac{(M^*+C_0^*)}{(1+C_0^*)}\right]^{-(1+NTU_\infty)} [-kT_1^*-NTU_\infty T_\infty^*+(1+NTU)] \quad .$$

Solving this expression for T^* gives

$$T^* = \frac{(1+NTU_\infty-kT_1^*-NTU_\infty T_\infty)\left(\frac{C_0^*+1}{C_0^*+M^*}\right)^{1+NTU_\infty} + kT_1^* + NTU_\infty T_\infty^*}{1+NTU_\infty} \quad .$$

This expression may be combined with the perfect gas law in order to obtain an expression for P^* as a function of M^*.

$$P^* = M^*\left[\frac{(1+NTU_\infty-kT_1^*-NTU_\infty T_\infty)\left(\frac{C_0^*+1}{C_0^*+M^*}\right)^{1+NTU_\infty} + kT_1^*+NTU_\infty T_\infty^*}{1+NTU_\infty}\right] \quad .$$

Table 1

Physical Dimensions of Experimental Apparatus

1. Test Receiver

   Volume: 1.03 cubic feet

   Internal Area: 5.61 square feet

   Nominal Internal Diameter: 10.19 inches

   Nominal Outside Diameter: 10.75 inches

   Nominal Internal Height: 21.75 inches

   Mass of the Receiver: 38.5 lbms.

   Material: 6061-T6 Aluminum

   Specific Heat: .226 Btu/lbm. °F

   Thermal Conductivity: 126 Btu/hr. ft. °F

2. Flow Metering Devices

   3/8 in. knife-edge orifice - discharge coeff. = .620

   1/8 in. nozzle - discharge coeff. = .858

   1/32 in. nozzle - discharge coeff. = .856

Table 2

Summary of High Flow Rate Runs

$C_0^* = 657$ $k = 1.4$ $T_1^* = 1.00$

Run No.	Total Run Time (sec)	Mass Flow Rate (lbm/sec)	Average NTU	Average % P* Deviation
1	1	.327	.123	7.93
2	1	.325	.092	8.11
3	1	.325	.104	5.59
4	1	.310	.101	7.47
5	1	.309	.089	6.93
6	1	.309	.085	6.11
7	1	.294	.121	10.06
8	1	.293	.084	5.58
9	1	.293	.084	4.92
10	1	.278	.102	6.93
11	1	.277	.105	7.35
12	1	.277	.115	9.63

Table 3

Summary of Low Flow Rate Runs

$C_0^* = 657$

Run No.	Total Run Time (sec)	Mass Flow Rate (lbm/sec)	Average NTU	Average % P* Deviation+
1	105	.0031	3.99	-2.61
2	105	.0031	2.86	-3.41
3	105	.0031	2.90	-3.18
4	105	.0029	3.69	-2.84
5	105	.0029	3.01	-3.11
6	105	.0029	4.78	-2.71
7	105	.0028	1.86	-3.68
8	105	.0028	3.49	-2.93
9	105	.0028	2.18	-3.39
10	105	.0024	2.92	-2.76
11	105	.0025	3.39	-2.65
12	105	.0025	5.54	-2.22
13	105	.0022	5.34	-2.50
14	105	.0022	7.78	-1.97
15	105	.0022	5.61	-2.09
16	105	.0018	4.52	-2.02
17	105	.0018	7.80	-1.67
18	105	.0019	4.43	-2.01
19	105	.0015	5.17	-1.70
20	105	.0015	8.00	-1.44
21	105	.0015	7.91	-1.27
22	105	.0012	4.89	-1.54
23	105	.0012	6.02	-1.33
24	105	.0012	3.83	-1.70
25	105	.0009	4.32	-1.43
26	105	.0009	6.01	-1.12
27	105	.0009	6.21	-1.07
28	105	.0007	4.58	-1.49
29	105	.0007	3.77	-1.36
30	105	.0007	3.47	-1.45
31	90	.0006	4.45	-1.07
32	90	.0006	13.88	-0.46
33	90	.0006	11.19	-0.52
34	75	.0004	14.49	-0.54
35	75	.0004	14.62	-0.54
36	75	.0004	12.39	-0.51

+A negative deviation indicates that the P* values predicted by Reynolds were lower than those actually observed.

Table 4

Summary of Isothermal Sink Runs

Run No.	Total Run Time (sec)	Mass Flow Rate (lbm/sec)	Average NTU	Average % P* Deviation+
1	150	.0031	2.69	-10.39
2	150	.0031	2.24	- 8.84
3	150	.0031	2.17	-11.08
4	150	.0028	2.07	-11.59
5	150	.0028	2.41	-10.35
6	150	.0028	1.97	-11.47
7	150	.0025	3.02	- 9.10
8	150	.0025	3.30	- 8.58
9	150	.0026	2.94	- 8.94
10	9	.0488	1.18	-13.32
11	9	.0478	1.41	-13.40
12	9	.0486	1.38	-13.22
13	9	.0420	1.39	-12.67
14	9	.0422	1.28	-13.37
15	9	.0422	1.15	-14.34
16	9	.0350	1.41	-12.49
17	9	.0348	1.03	-13.68
18	9	.0349	.94	-13.57
19	9	.0274	1.73	-10.78
20	9	.0272	1.13	-12.36
21	9	.0272	1.20	-12.47
22	9	.0194	1.85	- 9.92
23	8	.0192	1.09	-11.14
24	8	.0190	1.05	-11.14
25	7	.0111	1.29	- 7.68
26	7	.0111	1.20	- 7.85
27	7	.0114	1.15	- 7.98

+A negative deviation indicates that the P* values predicted by Reynolds were lower than those actually observed.

SCHEMATIC OF TEST RECEIVER

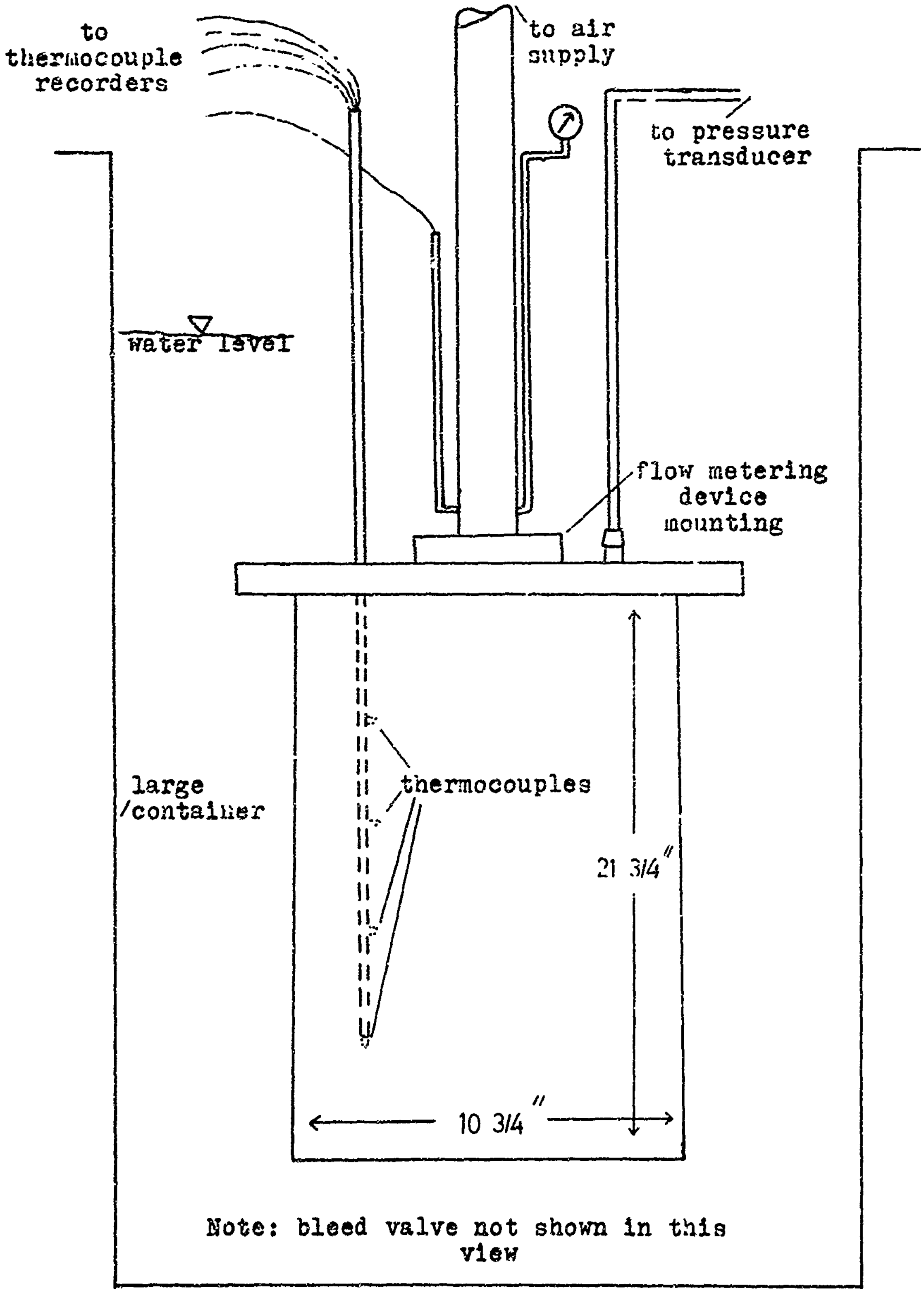

Fig. 1

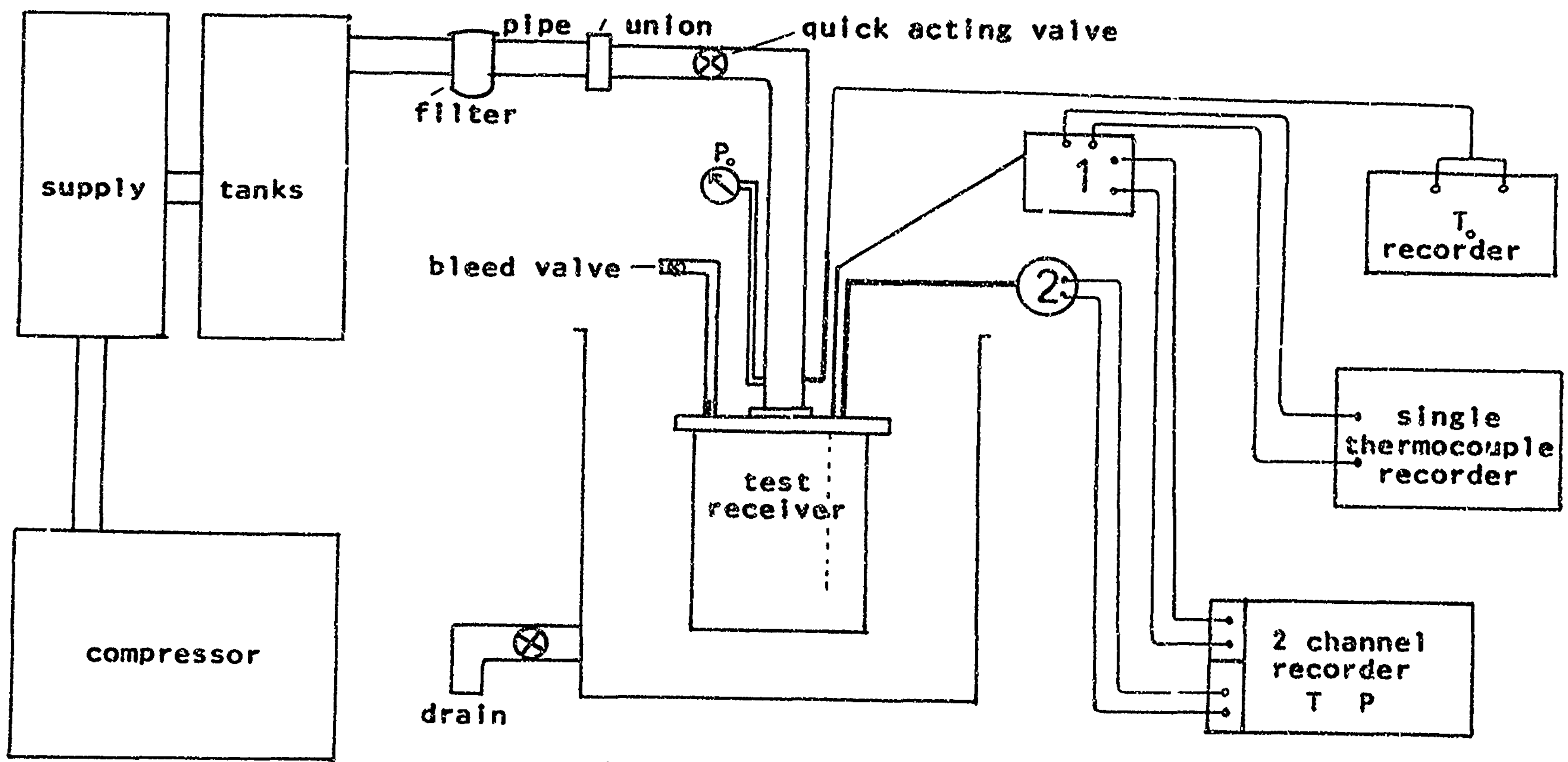

2-pressure transducer 1-thermocouple patch panel

TEST SYSTEM SCHEMATIC

Fig. 2

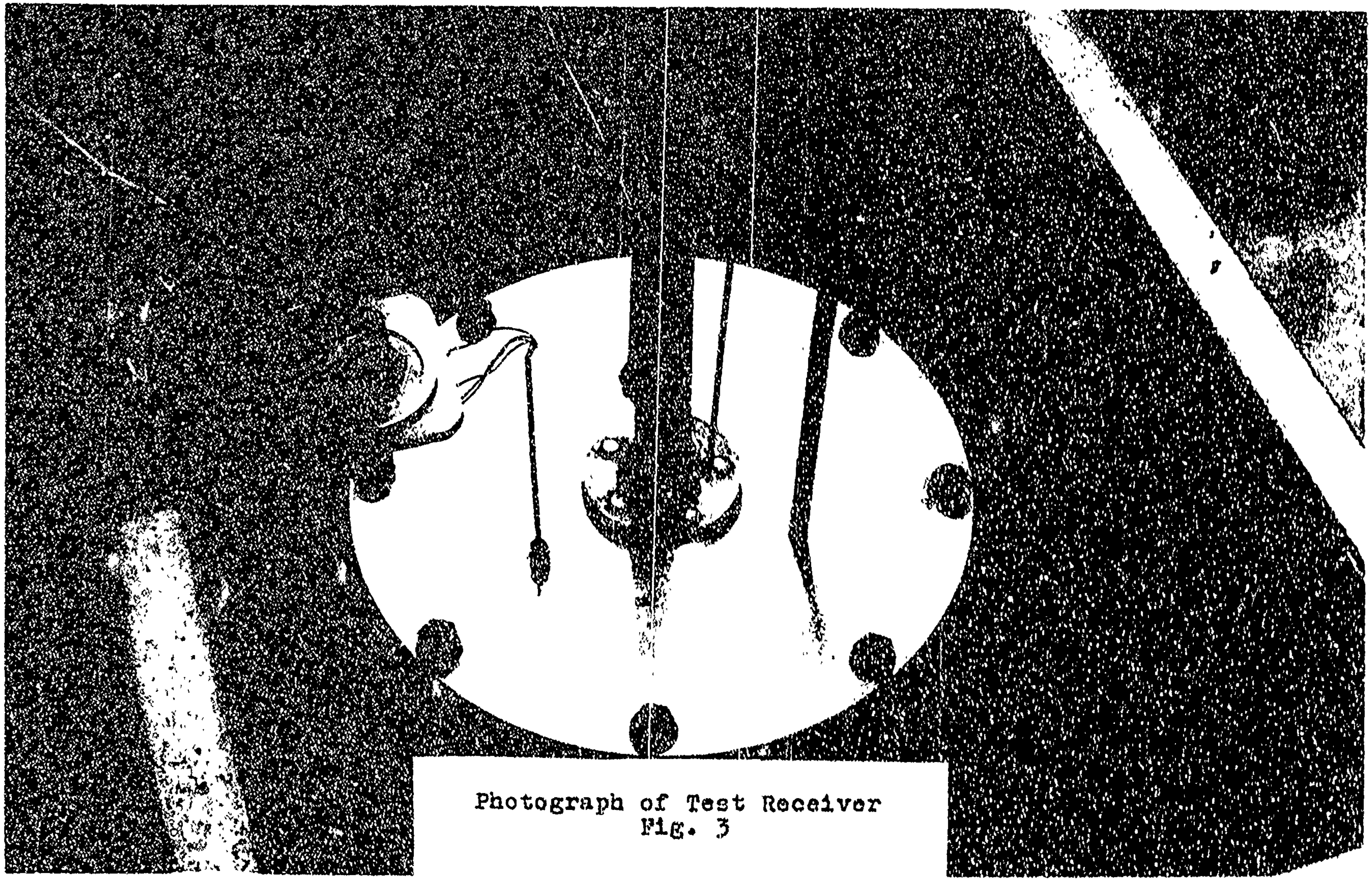

Photograph of Test Receiver
Fig. 3

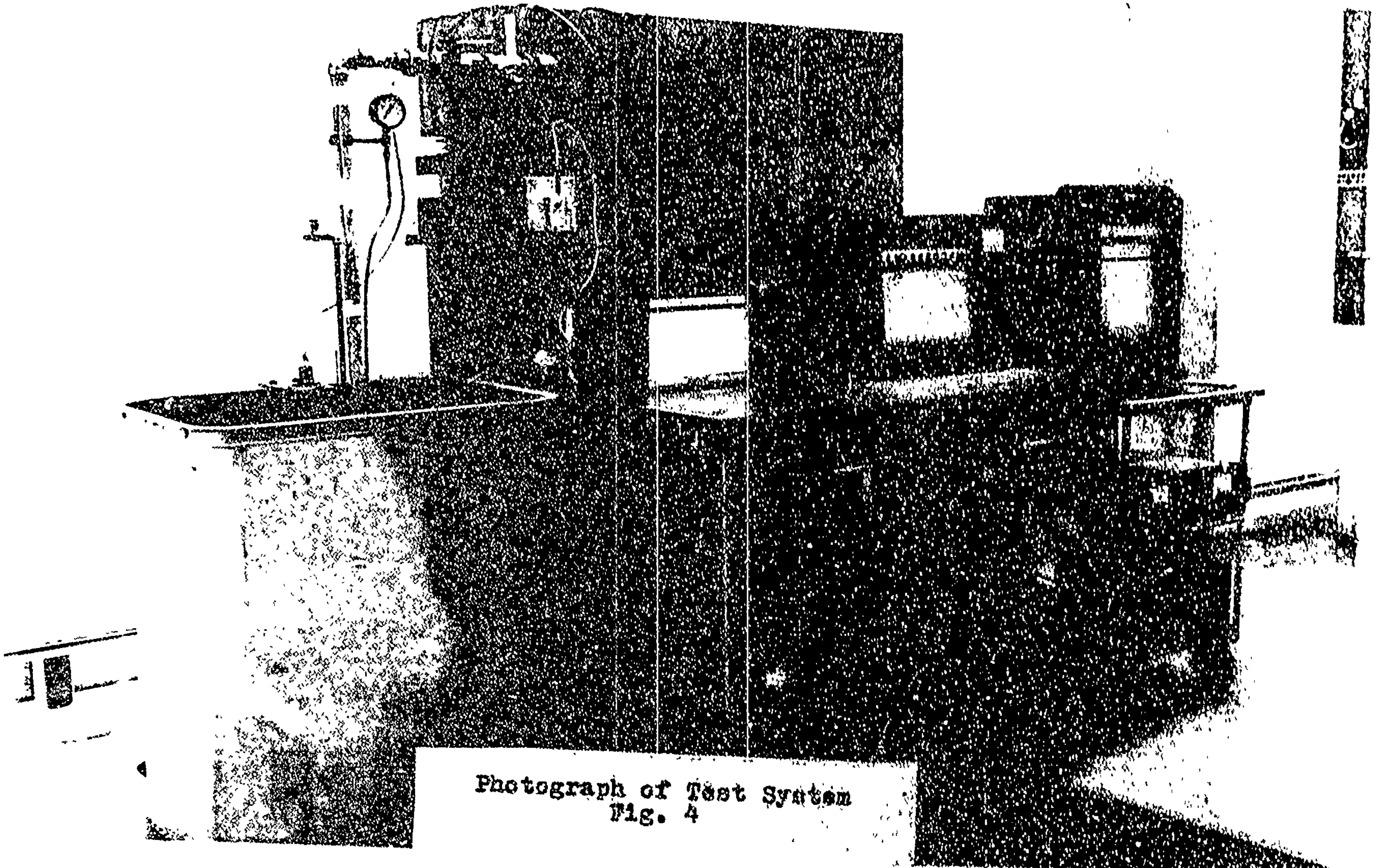

Photograph of Test System
Fig. 4

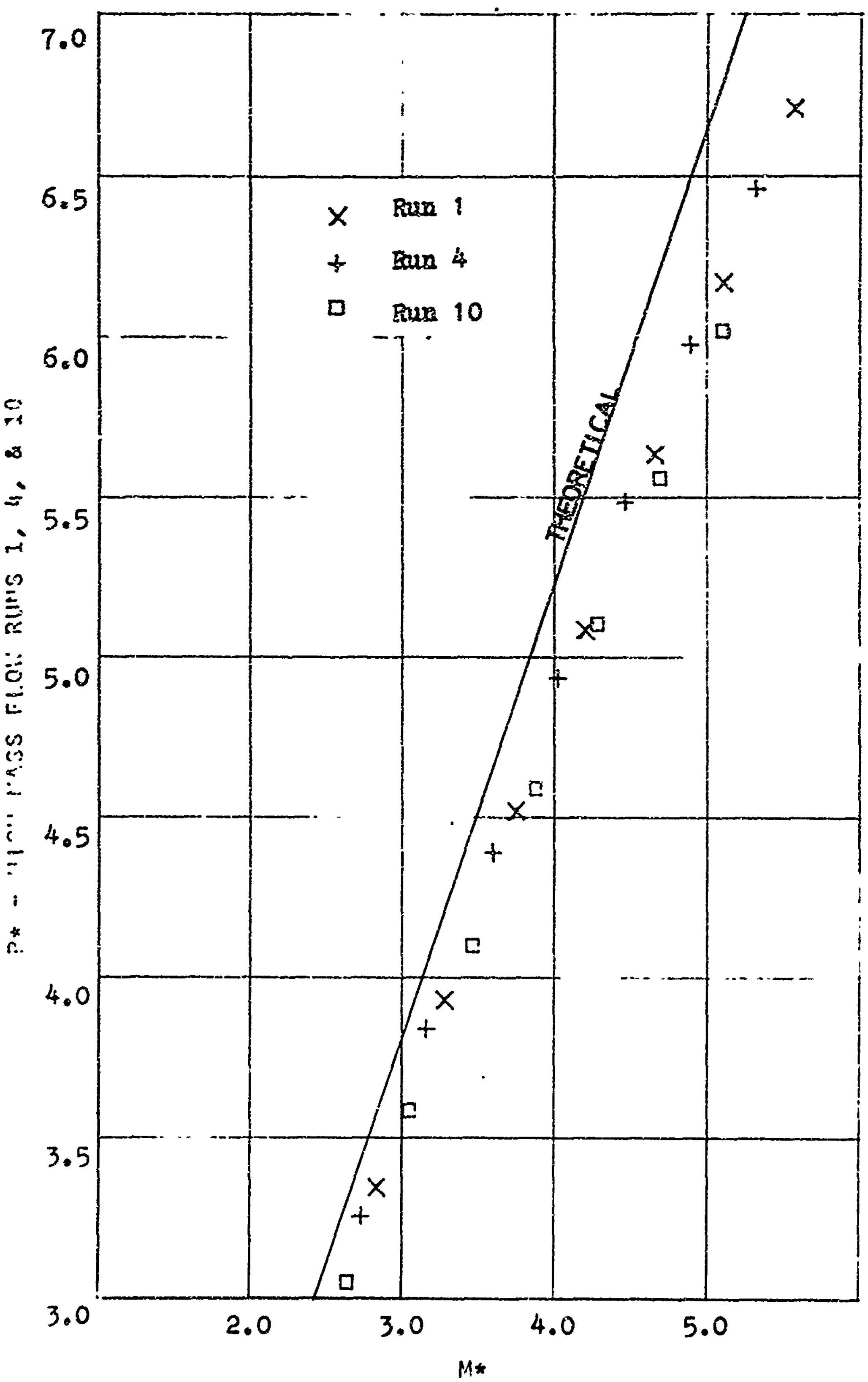
7.0
6.5
6.0
5.5
5.0
4.5
4.0
3.5
3.0
2.0
3.0
4.0
5.0
Run 1
Run 4
Run 10
THEORETICAL
M*

Fig. 5

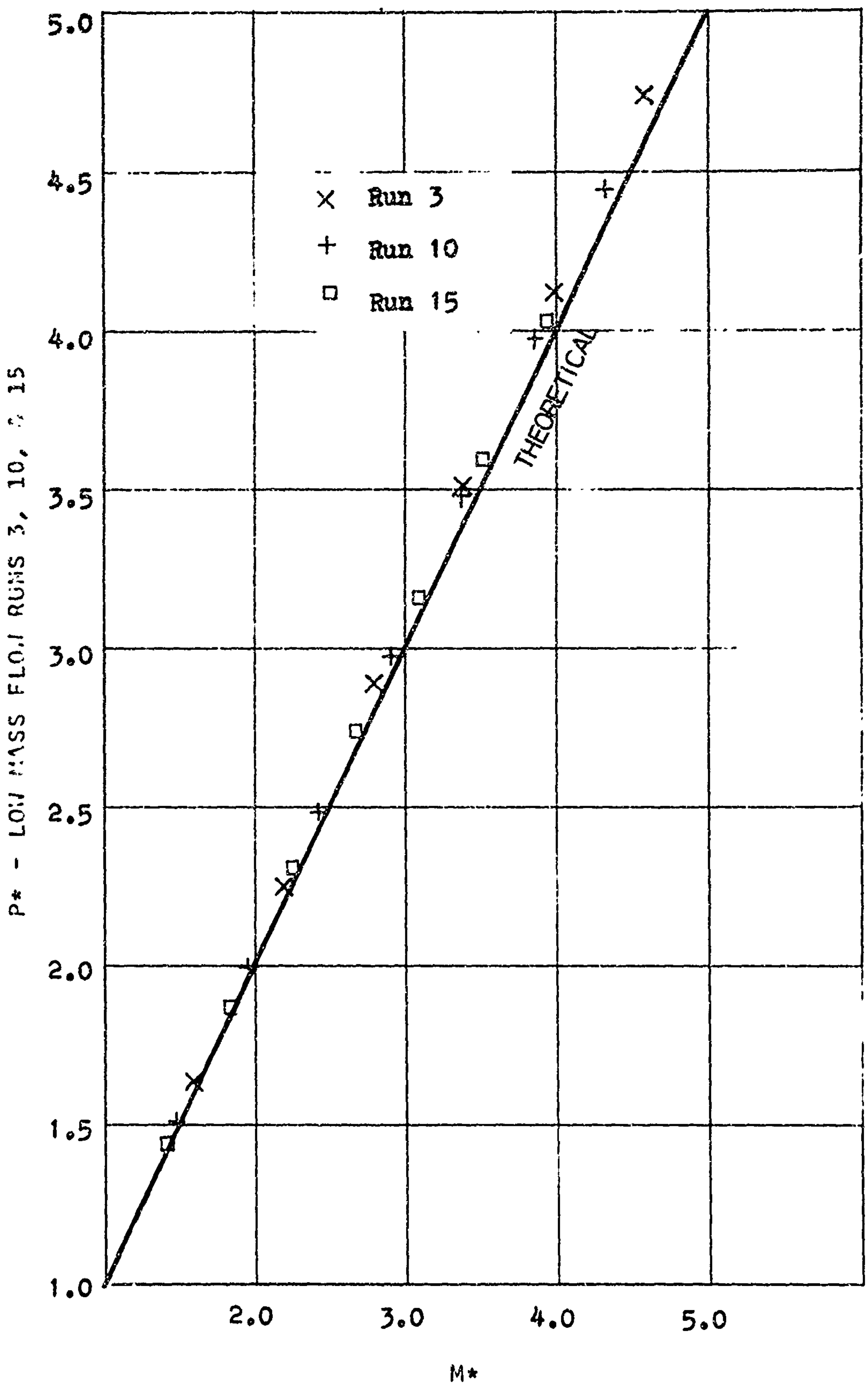
5.0
4.5
4.0
3.5
3.0
2.5
2.0
1.5
1.0
2.0
3.0
4.0
5.0
Run 3
Run 10
Run 15
THEORETICAL
P* - LOW MASS FLOW RUNS 3, 10, & 15
M*

Fig. 6

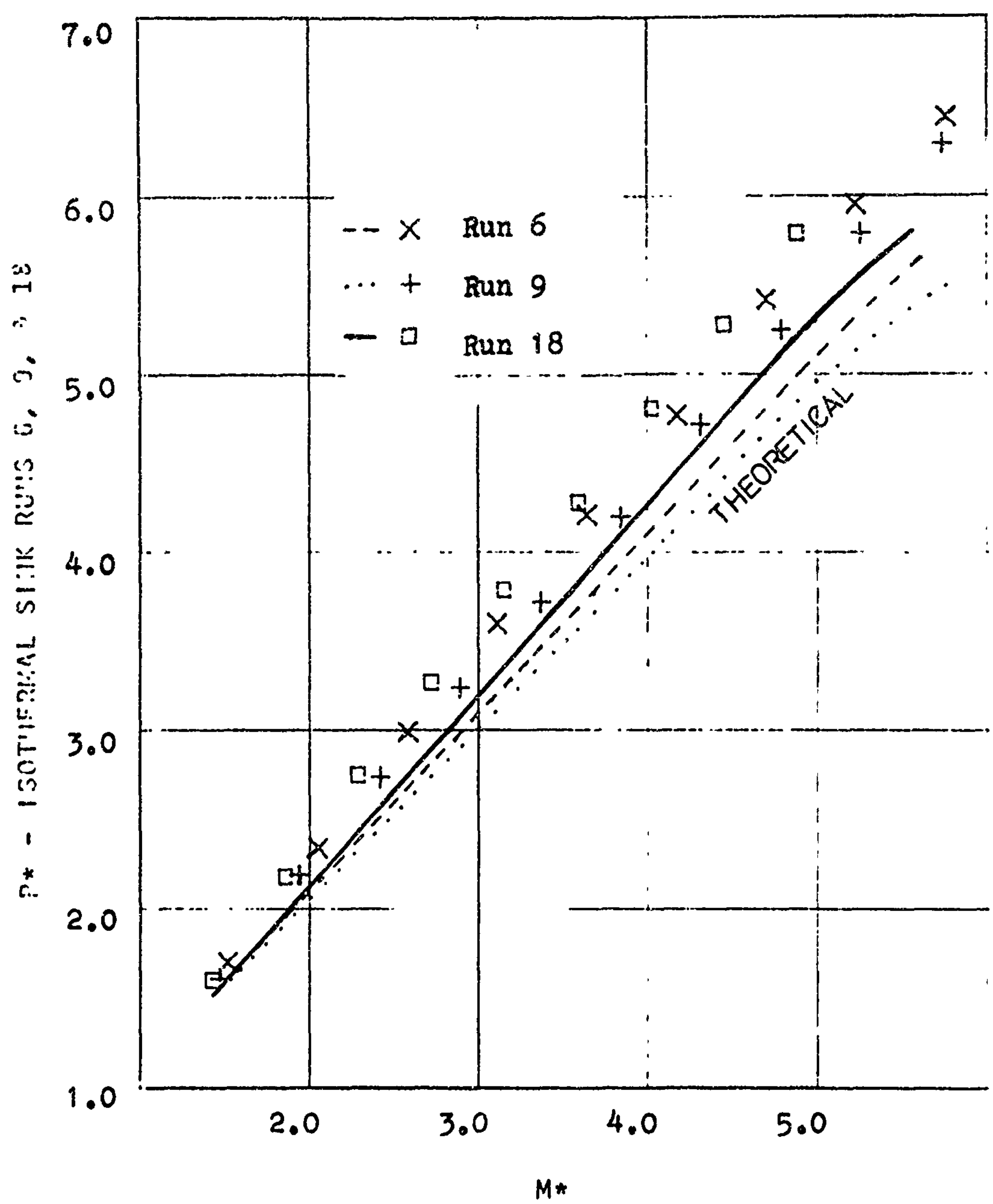

7.0
6.0
5.0
4.0
3.0
2.0
1.0
P* - ISOTHERMAL SINK RUNS 6, 9, & 18
Run 6
Run 9
Run 18
THEORETICAL
2.0
3.0
4.0
5.0
M*

Fig. 7

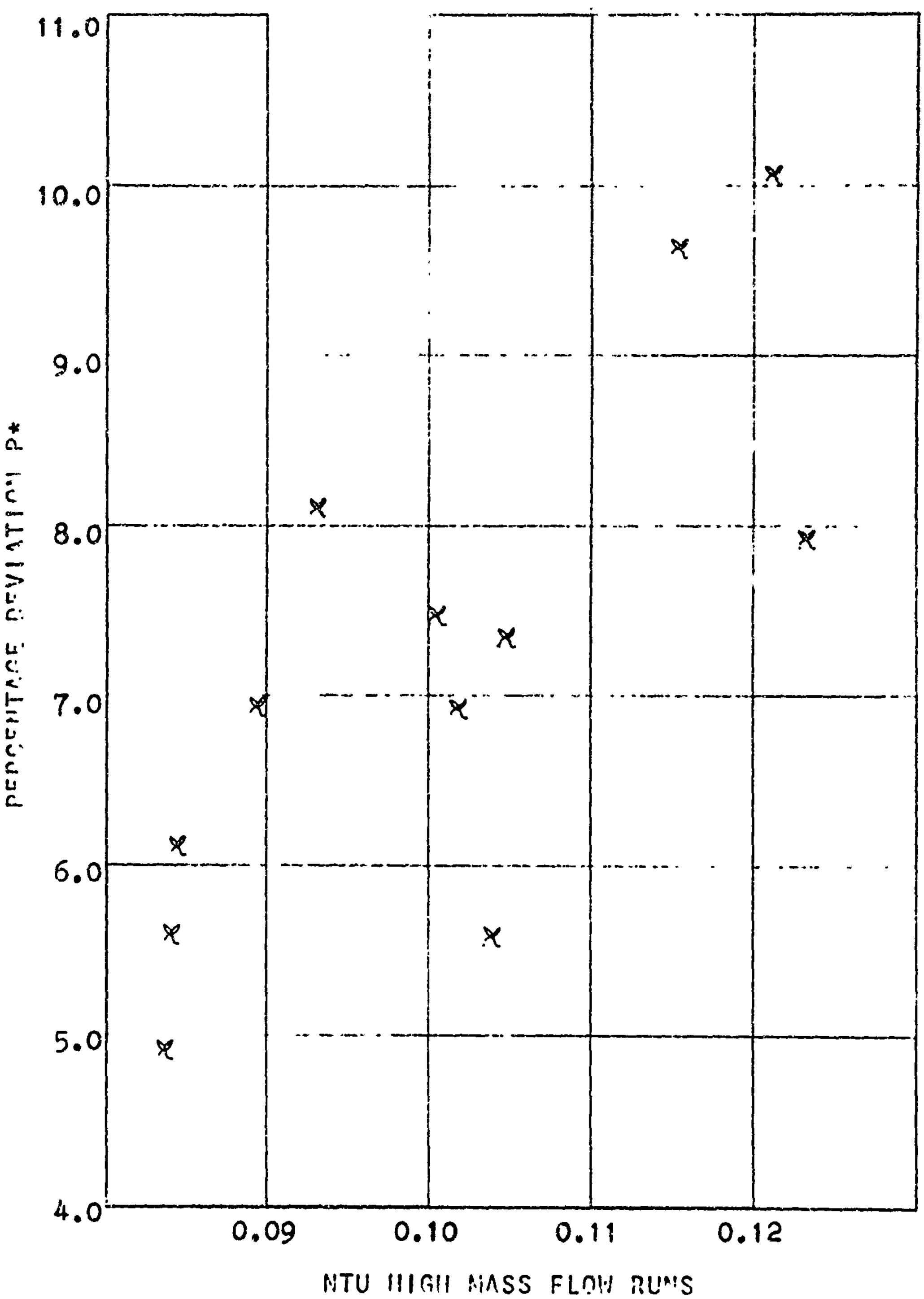
11.0
10.0
9.0
8.0
7.0
6.0
5.0
4.0
PERCENTAGE DEVIATION P*
0.09
0.10
0.11
0.12
NTU HIGH MASS FLOW RUNS

Fig. 8

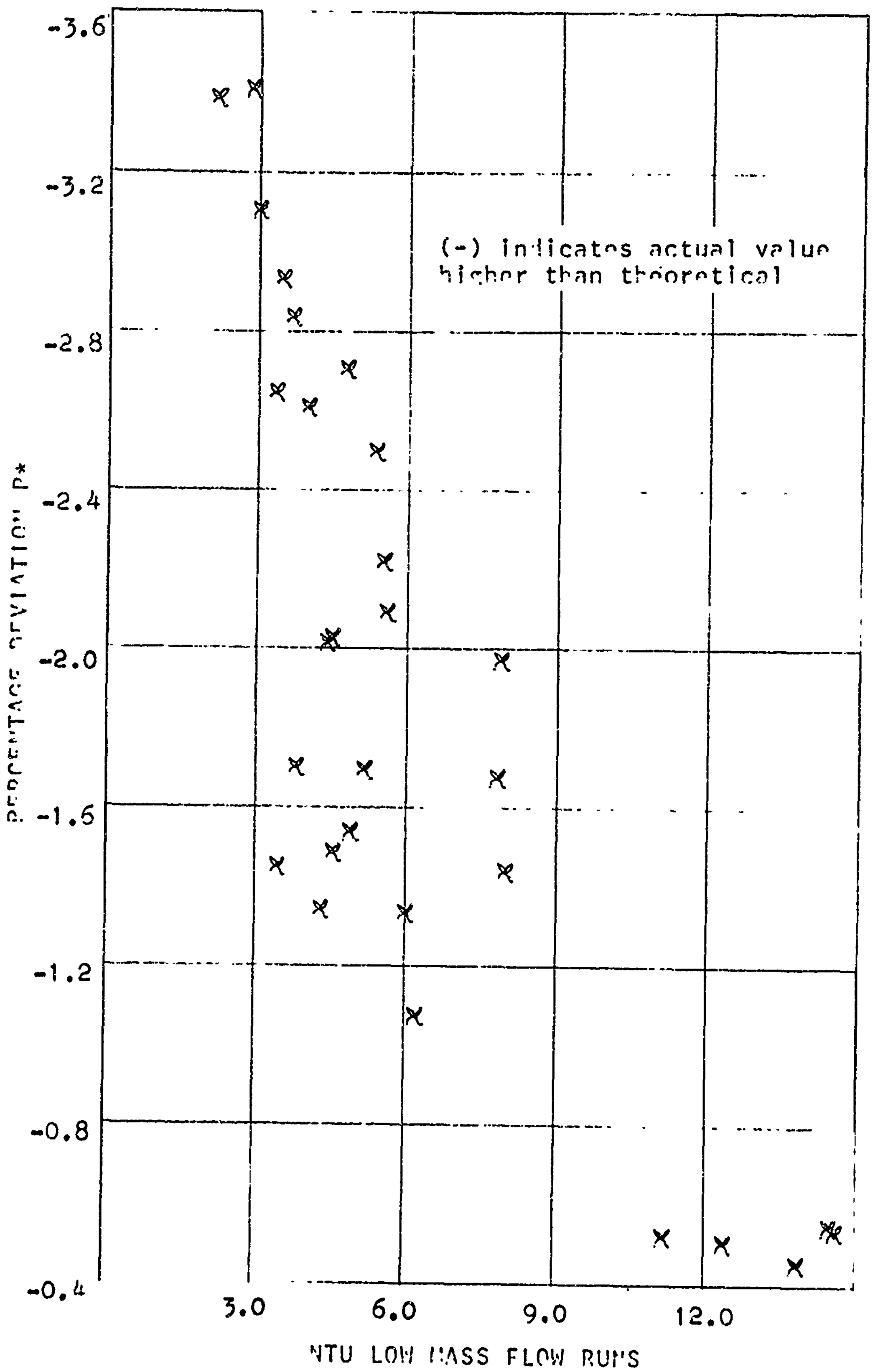
-3.6
-3.2
-2.8
-2.4
-2.0
-1.6
-1.2
-0.8
-0.4
3.0
6.0
9.0
12.0
PERCENTAGE DEVIATION D*
NTU LOW MASS FLOW RUNS
(-) Indicates actual value higher than theoretical

Fig. 9

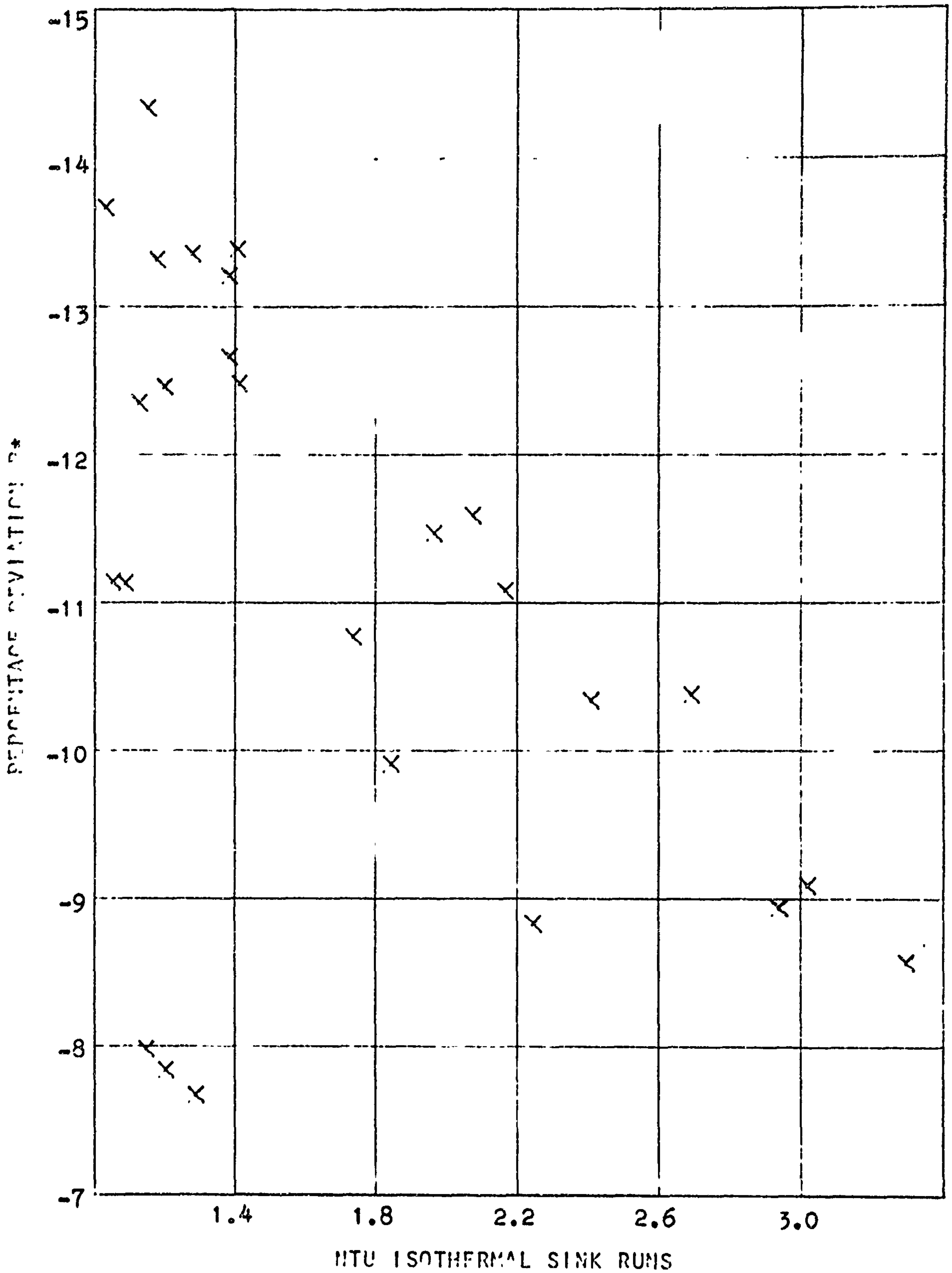
-15
-14
-13
-12
-11
-10
-9
-8
-7
PERCENTAGE DEVIATION P*
1.4
1.8
2.2
2.6
3.0
NTU ISOTHERMAL SINK RUNS

Fig. 10

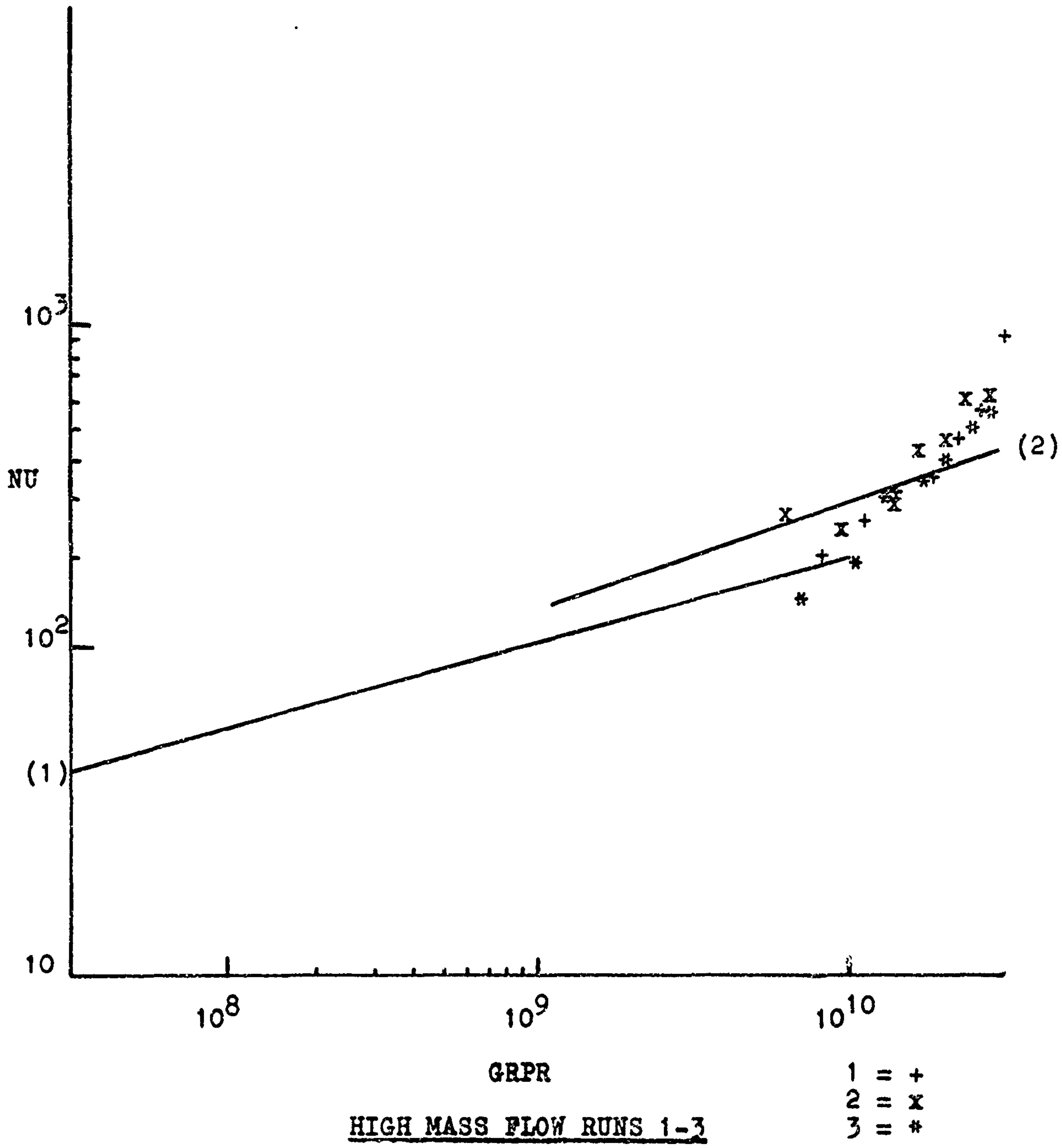

HIGH MASS FLOW RUNS 1-3

(1) laminar free convection line
(2) turbulent free convection line

Fig. 11

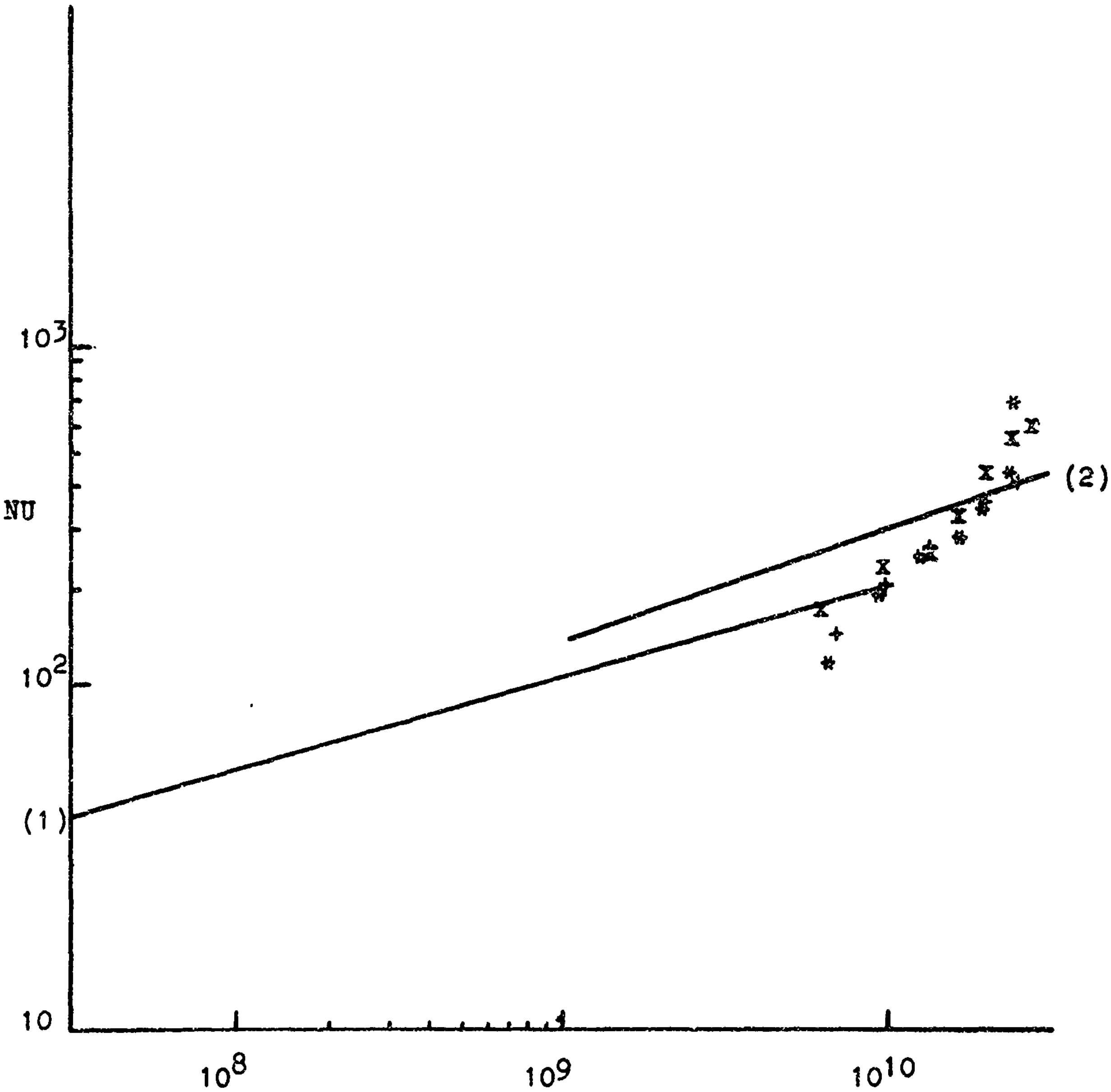

HIGH MASS FLOW RUNS 4-6

(1) laminar free convection line
(2) turbulent free convection line

Fig. 12

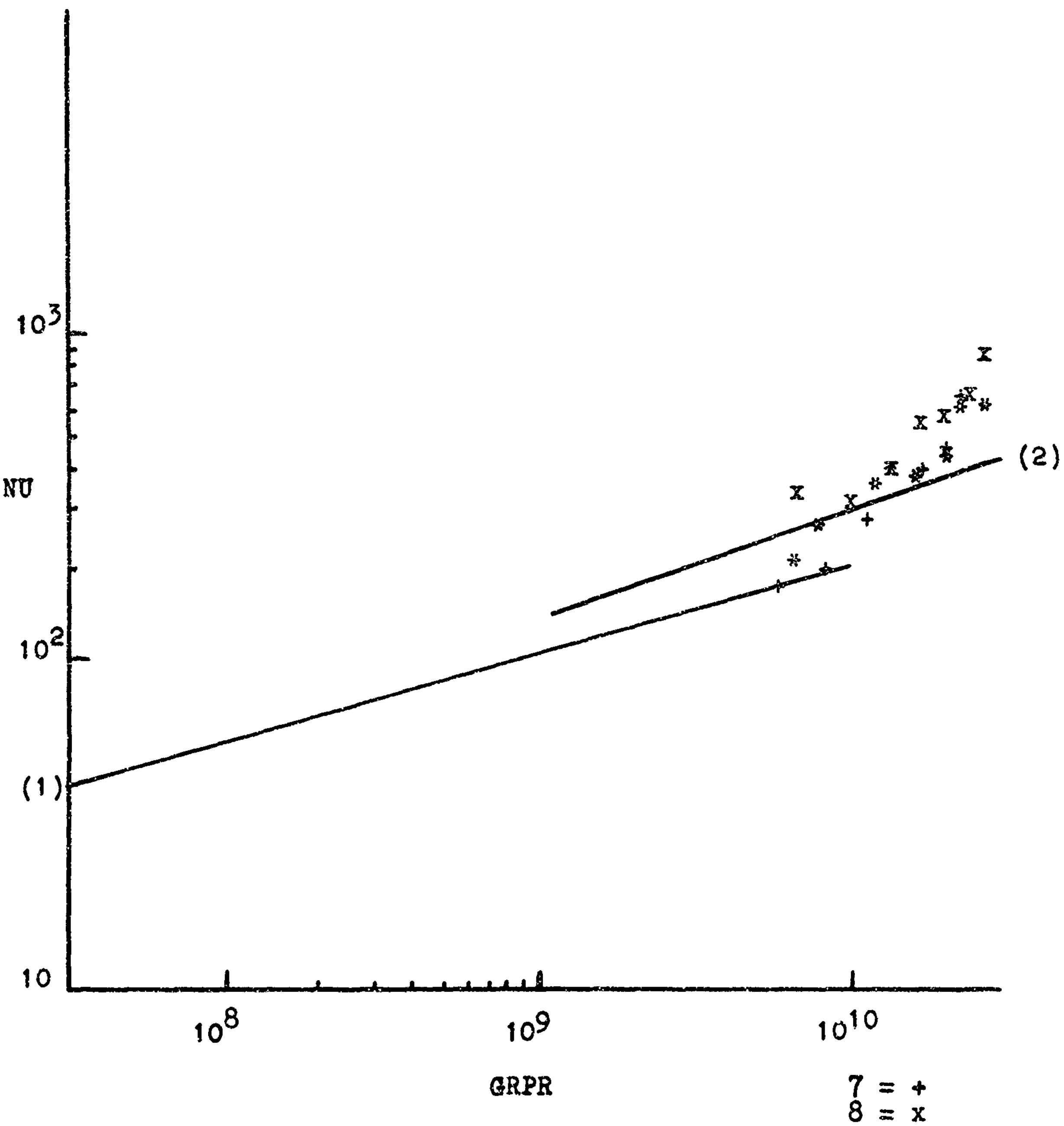

<u>HIGH MASS FLOW RUNS 7-9</u>

(1) laminar free convection line
(2) turbulent free convection line

Fig. 13

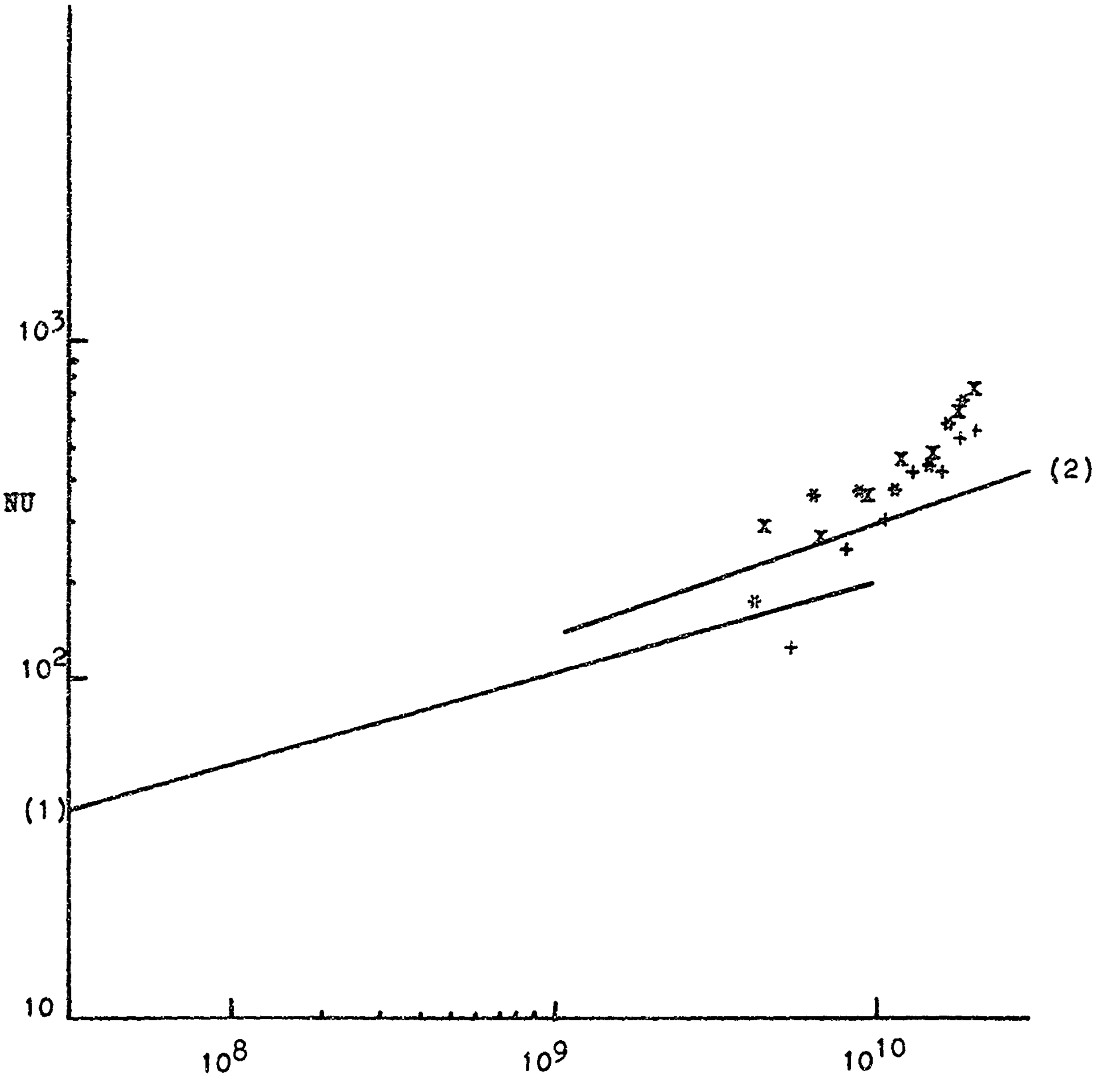

10 = +
11 = x
12 = *

HIGH MASS FLOW RUNS 10-12

(1) laminar free convection line
(2) turbulent free convection line

Fig. 14

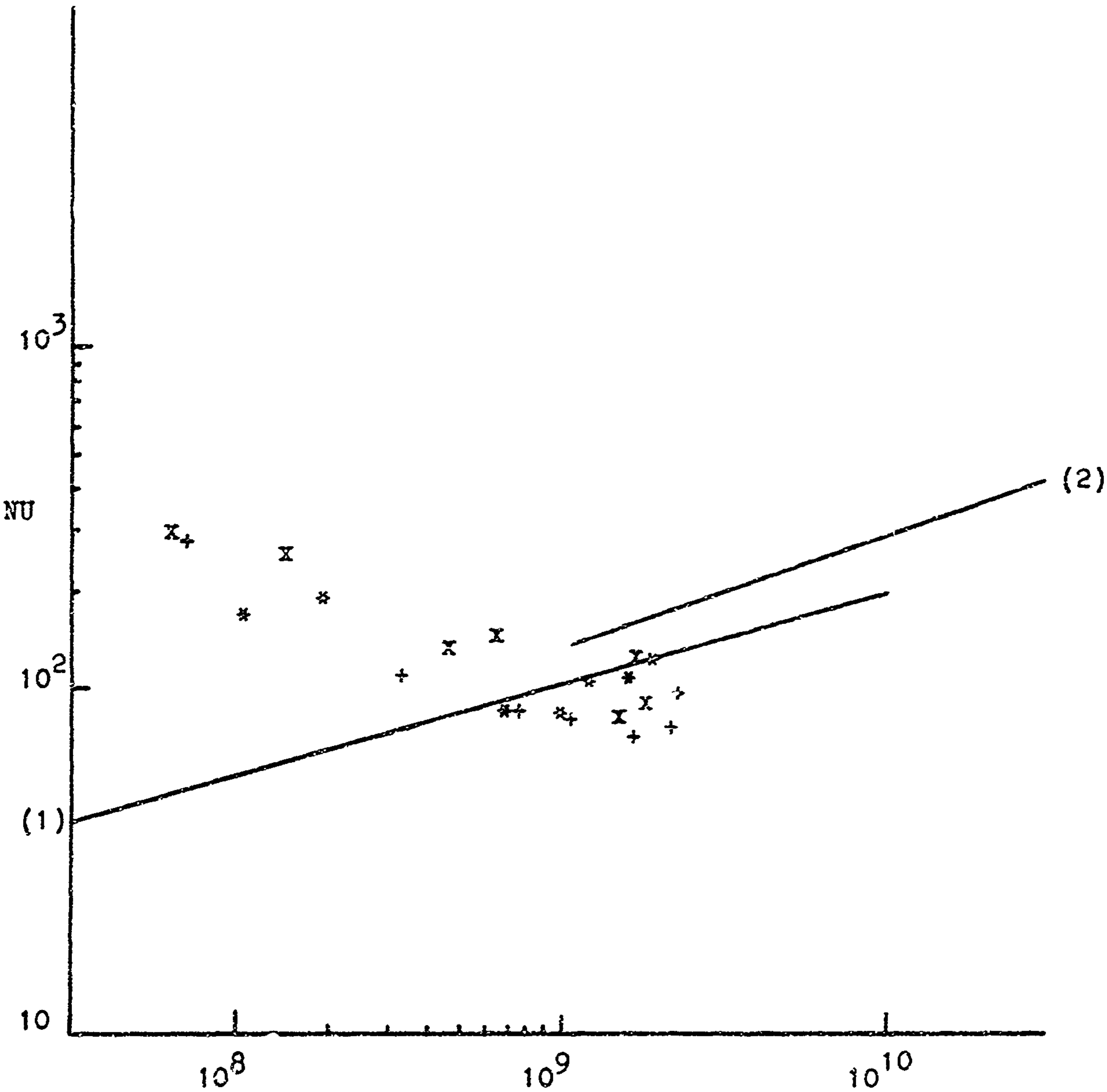

<u>LOW MASS FLOW RUNS 1-3</u>

(1) laminar free convection line
(2) turbulent free convection line

Fig. 15

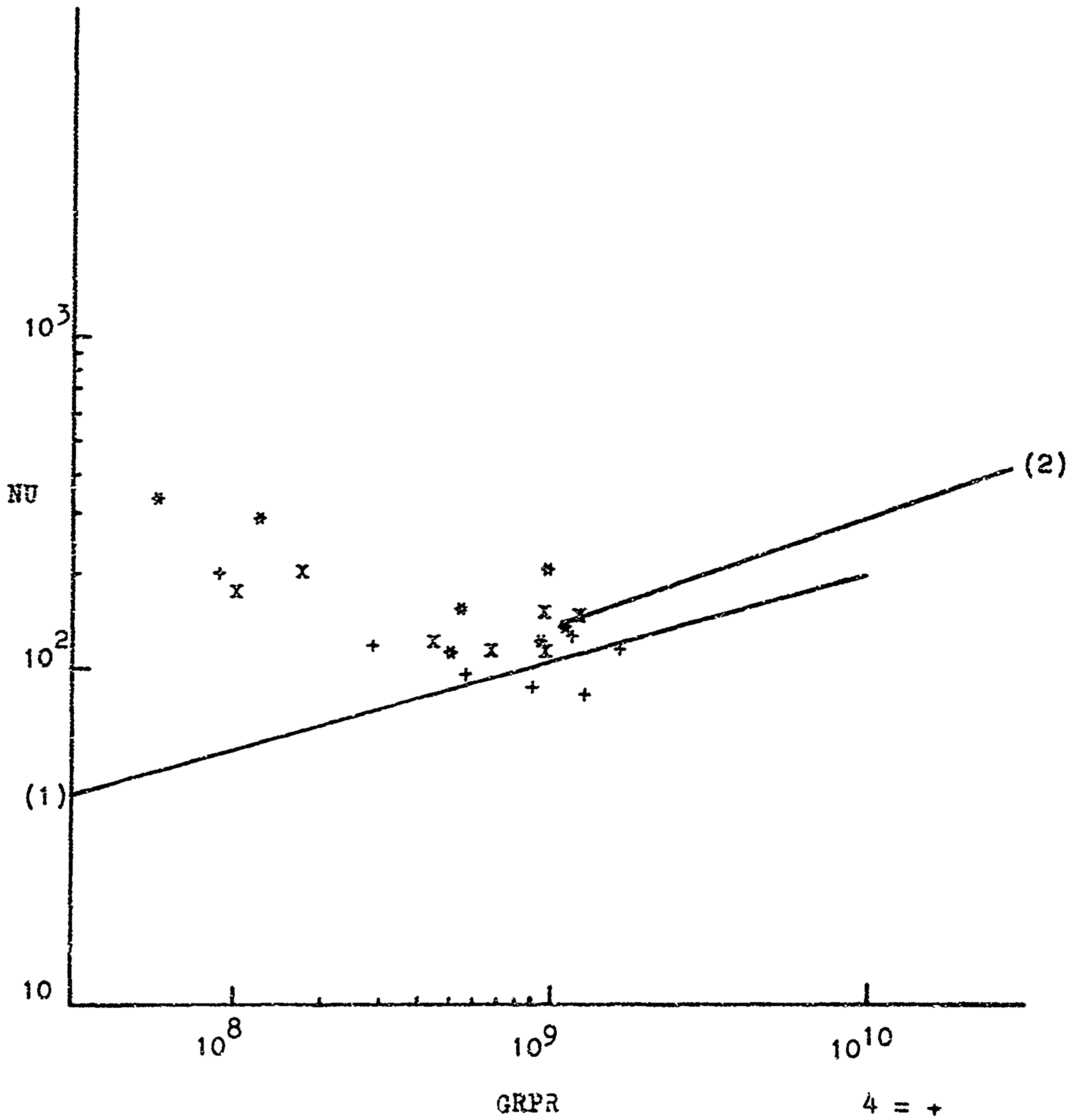

LOW MASS FLOW RUNS 4-6

(1) laminar free convection line
(2) turbulent free convection line

Fig. 16

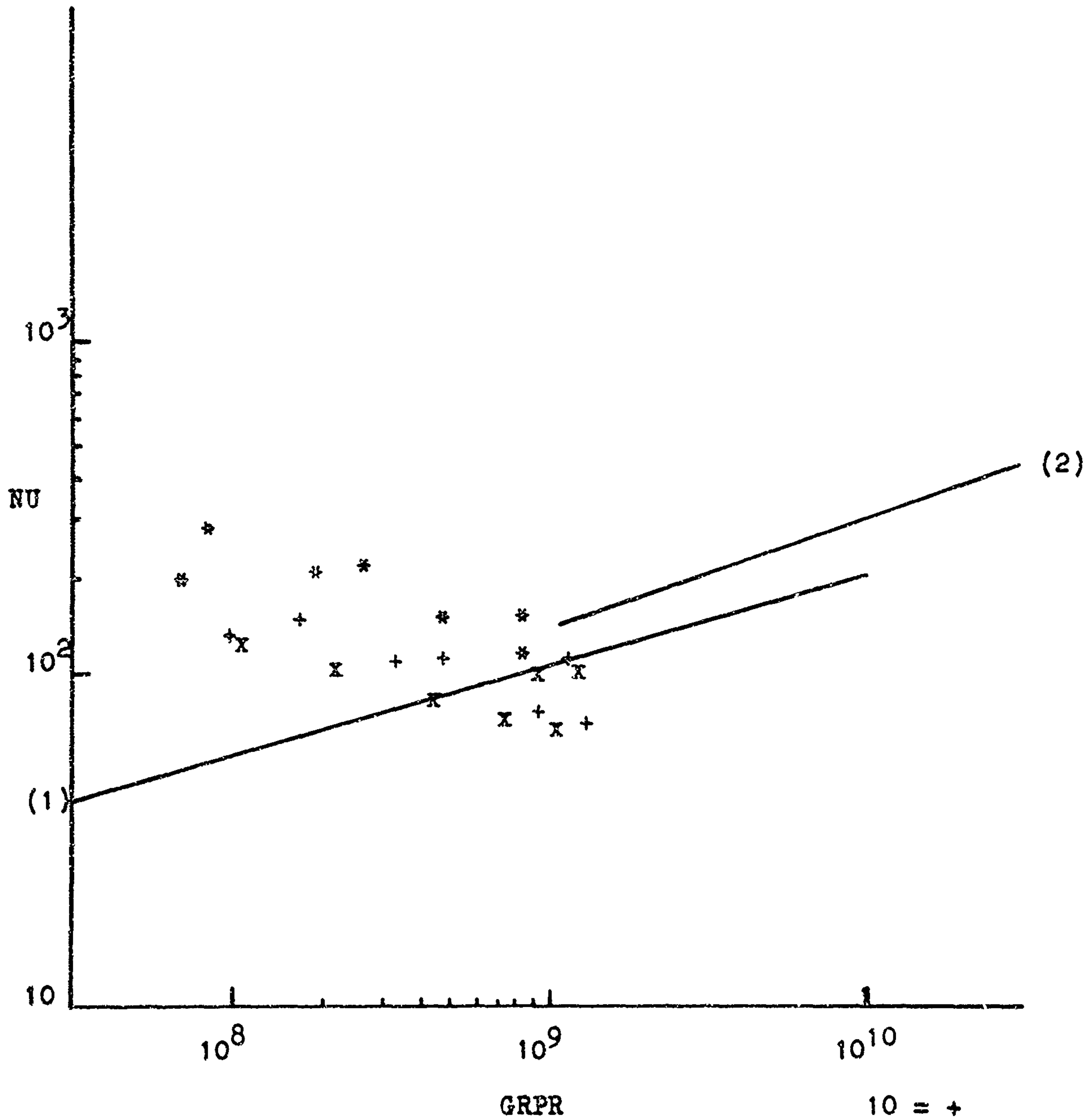

LOW MASS FLOW RUNS 10-12

(1) laminar free convection line
(2) turbulent free convection line

Fig. 17

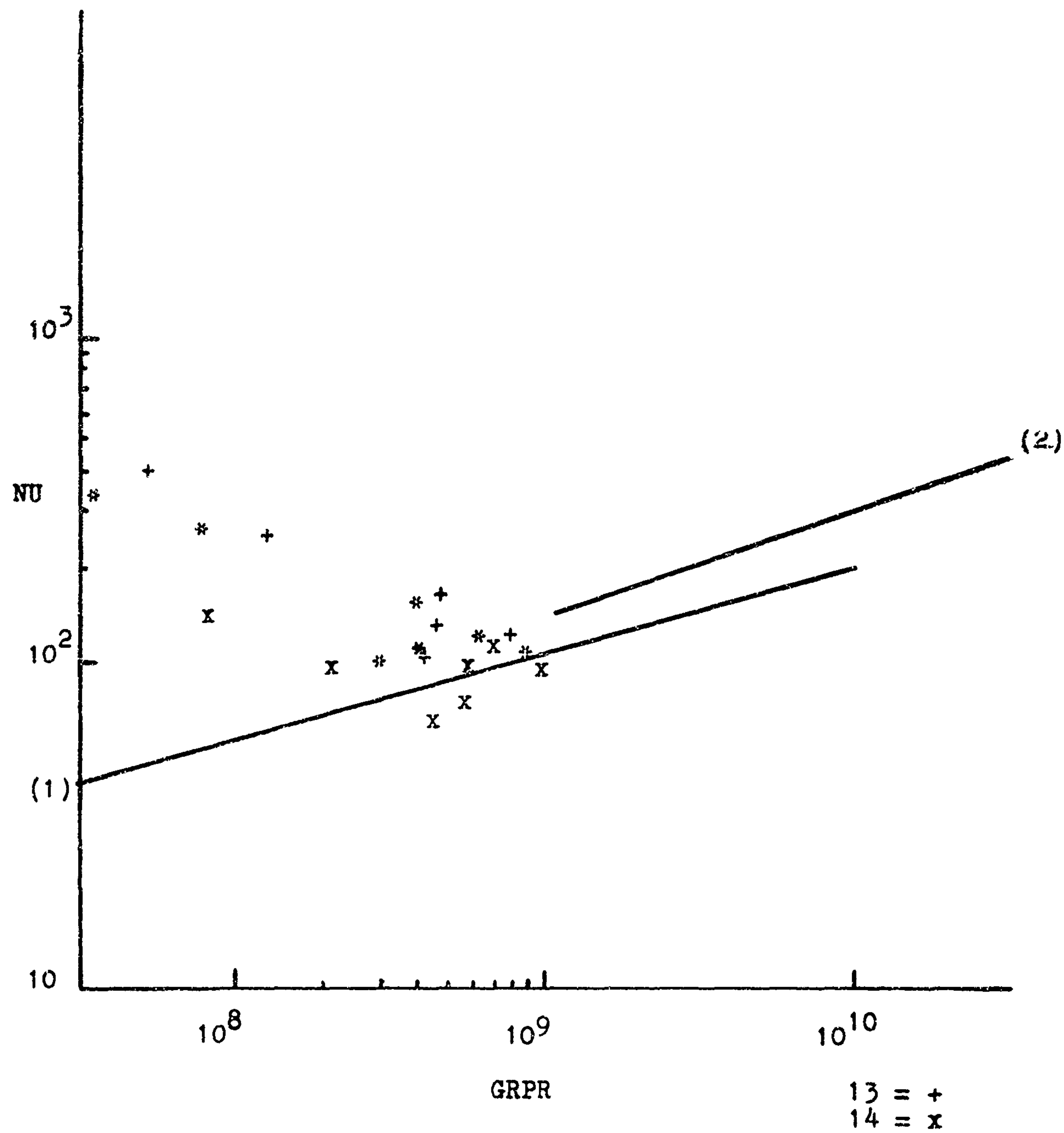

<u>LOW MASS FLOW RUNS 13-15</u>

(1) laminar free convection line
(2) turbulent free convection line

Fig. 18

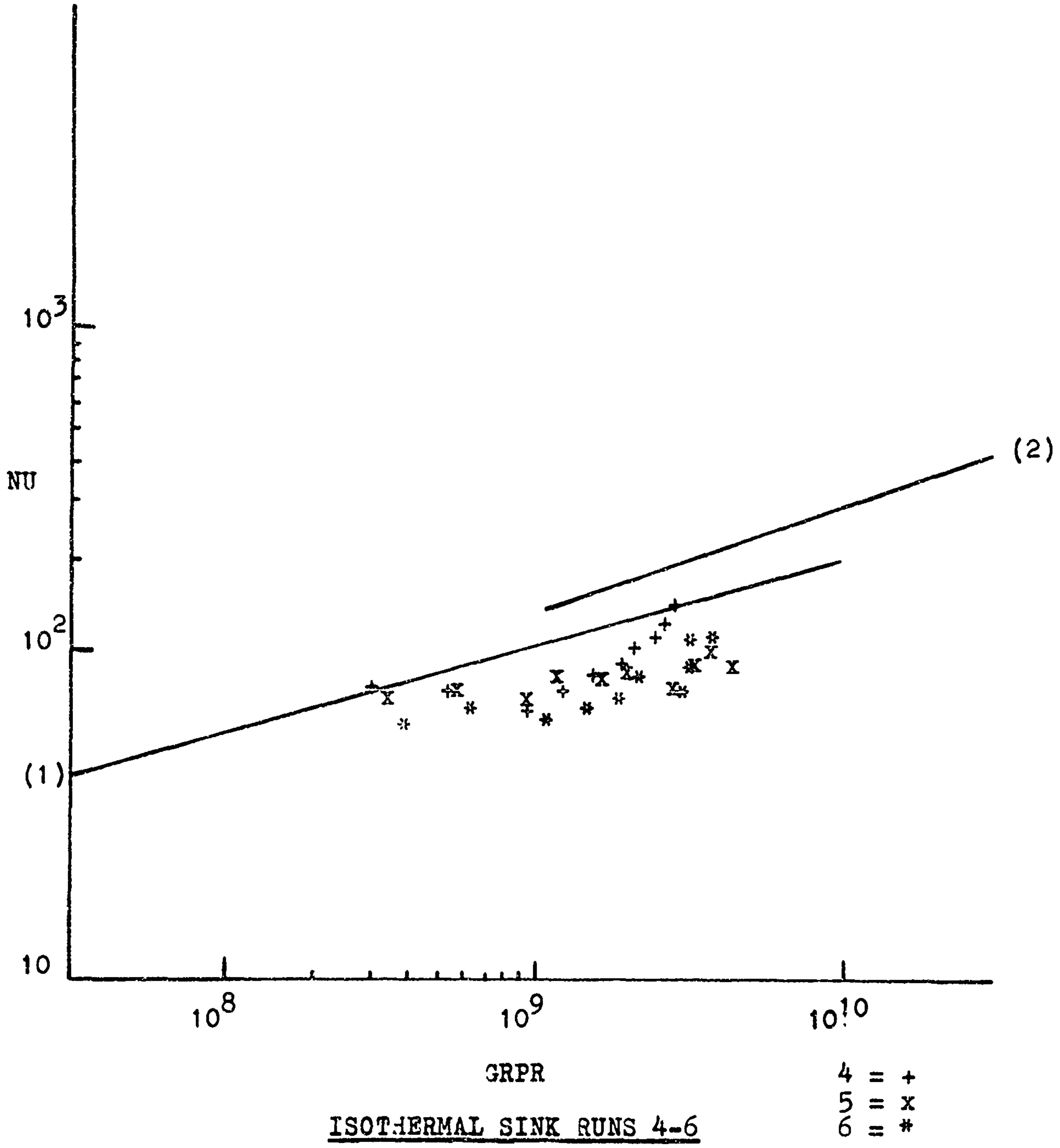

ISOTHERMAL SINK RUNS 4-6

(1) laminar free convection line
(2) turbulent free convection line

Fig. 19

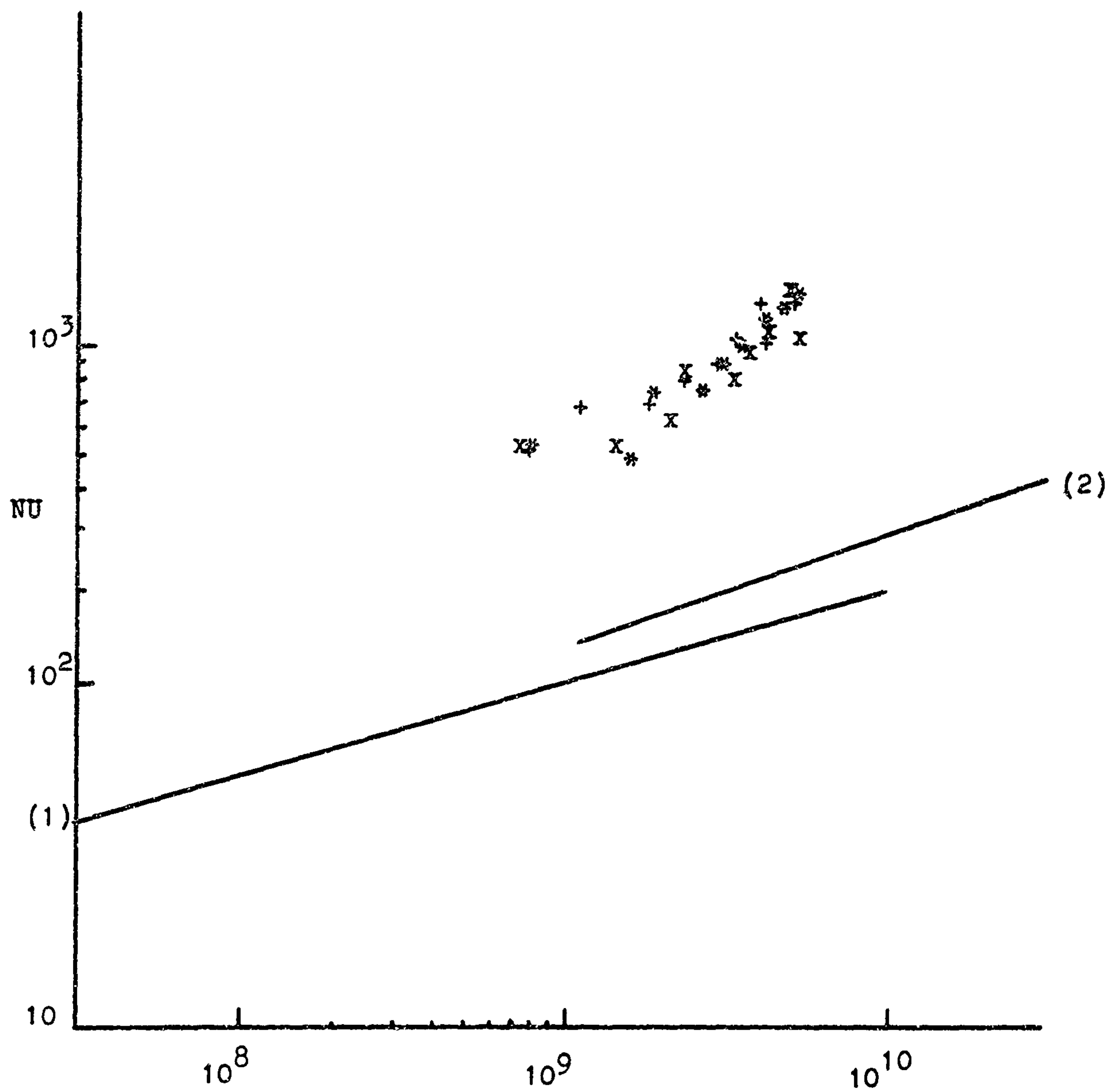

ISOTHERMAL SINK RUNS 10-12

(1) laminar free convection line
(2) turbulent free convection line

Fig. 20

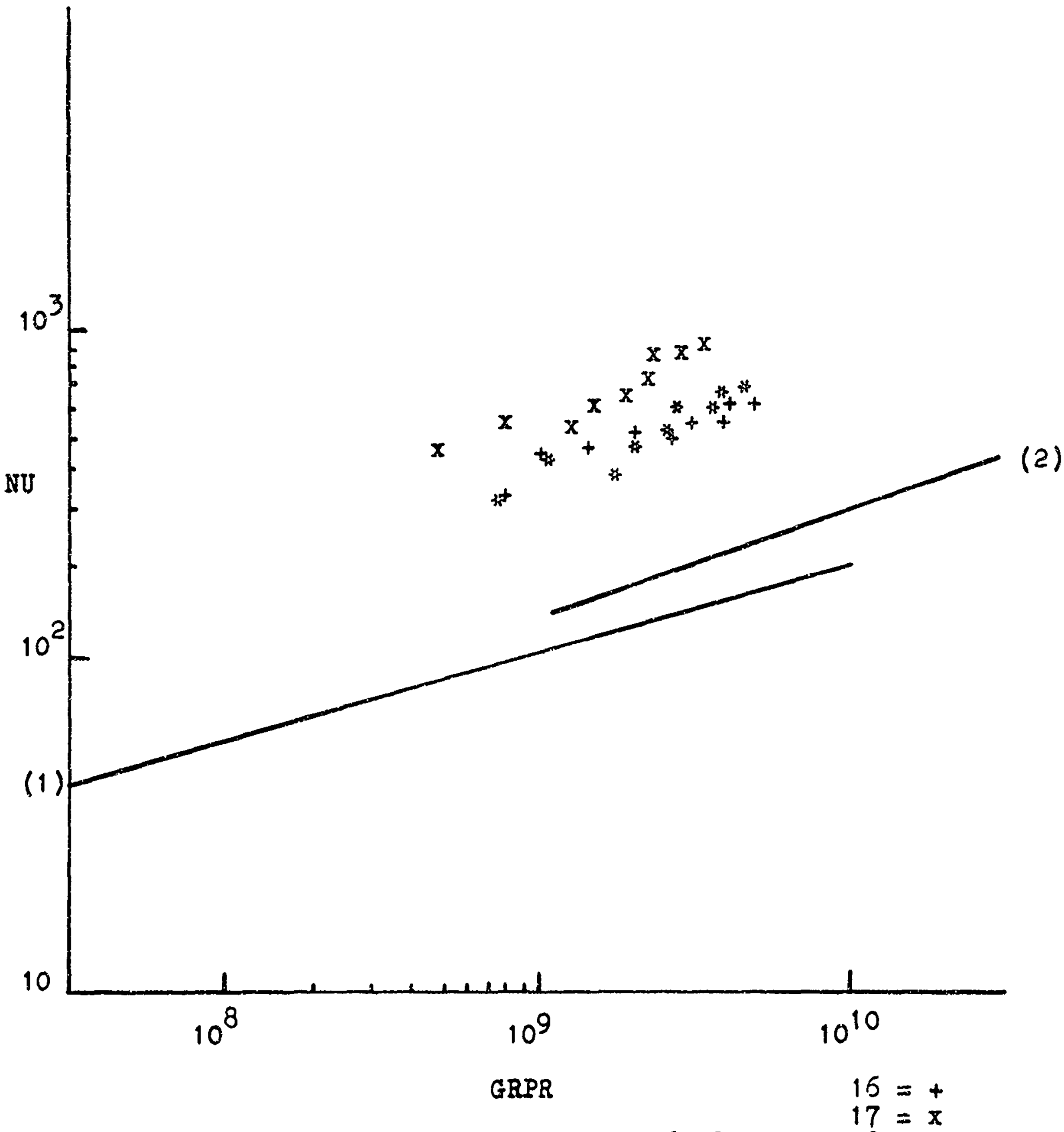

ISOTHERMAL SINK RUNS 16-18

(1) laminar free convection line
(2) turbulent free convection line

Fig. 21

LIST OF REFERENCES

1. Stanford Technical Report T-1, An Analytical Investigation of the Blowdown and Charging Process in a Single Gas Receiver, by W. C. Reynolds, October 1, 1955.

2. Stanford Technical Report T-2, An Experimental Investigation of Blowdown Process in a Single Gas Receiver, Including the Effects of Heat Transfer, by W. C. Reynolds, J. W. Millard, and W. M. Kays, December 1, 1956.

3. Grace, H. P. and Lapple, C. E., "Discharge Coefficients of Small Diameter Orifice and Flow Nozzles" Transactions of the ASME, v. 73, p. 639-647, July, 1951.

4. Carslaw, H. S. and Jaeger, J. D., Conduction of Heat in Solids, 2nd ed., 70-73, Clarendon Press, 1959.

5. Lyons, J. T., Pestorius, T. D., Sager, D. A., and von Suskil, J. D., Heat Transfer in Closed Containers with Gas Injection, Depart of Mech. Eng. NPGS, Monterey, California, December, 1968.

6. Ulrich, R. D., Wirtz, D. P., and Nunn, R. H., Thermal Analysis of Gas Pressurized Expulsion System: Part I: Heat Transfer in Closed Containers with Gas Injection, Naval Weapons Center, China Lake, California, 1968.

Unclassified
Security Classification

DOCUMENT CONTROL DATA - R & D	
(Security classification of title, body of abstract and indexing annotation must be entered when the overall report is classified)	
1. ORIGINATING ACTIVITY (Corporate author) Naval Postgraduate School Monterey, California 93940	2a. REPORT SECURITY CLASSIFICATION Unclassified
	2b. GROUP
3. REPORT TITLE Heat Transfer Considerations in a Pressure Vessel Being Charged	
4. DESCRIPTIVE NOTES (Type of report and inclusive dates) Master's Thesis; (June 1969)	
5. AUTHOR(S) (First name, middle initial, last name) John Thomas Lyons III	

6. REPORT DATE	7a. TOTAL NO. OF PAGES	7b. NO. OF REFS
June 1969	102	6

8a. CONTRACT OR GRANT NO.	9a. ORIGINATOR'S REPORT NUMBER(S)
b. PROJECT NO.	
c.	9b. OTHER REPORT NO(S) (Any other numbers that may be assigned this report)
d.	

10. DISTRIBUTION STATEMENT

Distribution of this document is unlimited.

11. SUPPLEMENTARY NOTES	12. SPONSORING MILITARY ACTIVITY
	Naval Postgraduate School Monterey, California 93940

13. ABSTRACT

Experimental data for the charging of an air receiver is presented and interpreted in detail. The data indicates a substantial departure from the adiabatic behavior. The experimental results are used to evaluate existing closed form expressions for the thermodynamic state of a gas in a receiver. A method for experimentally determining the convective heat transfer coefficient is developed, evaluated and used in conjunction with these expressions.

The experimental work was performed from March 1969 through May 1969 at the Naval Postgraduate School, Monterey, California.

DD FORM 1 NOV 65 1473 (PAGE 1)

S/N 0101-807-6811

Unclassified
Security Classification

A-31408

14 KEY WORDS	LINK A		LINK B		LINK C	
	ROLE	WT	ROLE	WT	ROLE	WT
Convective Heat Transfer						
Charging of Receiver						
Thermodynamic State of a Gas						